

RESEARCH ARTICLE

Minimal SPI1-T3SS effector requirement for *Salmonella* enterocyte invasion and intracellular proliferation *in vivo*

Kaiyi Zhang¹, Ambre Riba¹, Monika Nietschke², Natalia Torow¹, Urska Repnik³, Andreas Pütz¹, Marcus Fulde⁴, Aline Dupont¹, Michael Hensel², Mathias Hornef^{1*}

1 Institute of Medical Microbiology, RWTH University Hospital, Aachen, Germany, **2** Division of Microbiology, University of Osnabrück, Osnabrück, Germany, **3** Department of Biosciences, University of Oslo, Oslo, Norway, **4** Institute of Microbiology and Epizootics, Freie Universität Berlin, Berlin, Germany

* mhornef@ukaachen.de



OPEN ACCESS

Citation: Zhang K, Riba A, Nietschke M, Torow N, Repnik U, Pütz A, et al. (2018) Minimal SPI1-T3SS effector requirement for *Salmonella* enterocyte invasion and intracellular proliferation *in vivo*. PLoS Pathog 14(3): e1006925. <https://doi.org/10.1371/journal.ppat.1006925>

Editor: Andreas J. Baumler, University of California Davis School of Medicine, UNITED STATES

Received: October 27, 2017

Accepted: February 6, 2018

Published: March 9, 2018

Copyright: © 2018 Zhang et al. This is an open access article distributed under the terms of the [Creative Commons Attribution License](https://creativecommons.org/licenses/by/4.0/), which permits unrestricted use, distribution, and reproduction in any medium, provided the original author and source are credited.

Data Availability Statement: All relevant data are within the paper and its Supporting Information files.

Funding: This work was supported by: German Research Foundation (<http://www.dfg.de/en/>) Priority Program 1580 “Intracellular Compartments as Places of Pathogen - Host Interaction” to MWH and MH, the German Research Foundation Individual Grant Ho-2236/12-1, Ho-2236/8-1 and Ho-2236/14-1 to MHo, the German Research Foundation Individual Grant HE1964/18-2 and the

Abstract

Effector molecules translocated by the *Salmonella* pathogenicity island (SPI)1-encoded type 3 secretion system (T3SS) critically contribute to the pathogenesis of human *Salmonella* infection. They facilitate internalization by non-phagocytic enterocytes rendering the intestinal epithelium an entry site for infection. Their function *in vivo* has remained ill-defined due to the lack of a suitable animal model that allows visualization of intraepithelial *Salmonella*. Here, we took advantage of our novel neonatal mouse model and analyzed various bacterial mutants and reporter strains as well as gene deficient mice. Our results demonstrate the critical but redundant role of SopE₂ and SipA for enterocyte invasion, prerequisite for transcriptional stimulation and mucosal translocation *in vivo*. In contrast, the generation of a replicative intraepithelial endosomal compartment required the cooperative action of SipA and SopE₂ or SipA and SopB but was independent of SopA or host MyD88 signaling. Intraepithelial growth had no critical influence on systemic spread. Our results define the role of SPI1-T3SS effector molecules during enterocyte invasion and intraepithelial proliferation *in vivo* providing novel insight in the early course of *Salmonella* infection.

Author summary

Non-typhoidal *Salmonella* represent a major causative agent of gastroenteritis worldwide. Hallmark of the pathogenesis is their ability to actively invade the intestinal epithelium by virtue of their type 3 secretion system that delivers bacterial virulence factors directly into the host cell cytosol. The role of these virulence factors during enterocyte entry and intraepithelial growth has only been investigated *in vitro* since the previously established *in vivo* models in small animals did not allow visualization of intraepithelial *Salmonella*. However, immortalized cell lines lack the overlaying mucus layer, final cell lineage differentiation, apical-basolateral polarization as well as continuous migration along the crypt villus axis and thus the role of virulence factors during the *Salmonella* infection *in vivo* has remained largely undefined. Here, we took advantage of our novel neonatal mouse infection model

Collaborative Research Center SFB 944 (P4) to MHe, and the German Research Foundation Individual Grant To-1052/1-1 to NT. The funders had no role in study design, data collection and analysis, decision to publish, or preparation of the manuscript.

Competing interests: The authors have declared that no competing interest exists.

and for the first time systematically analyzed the importance of *Salmonella* virulence factors for enterocyte invasion and intraepithelial growth.

Introduction

Non-typhoidal *Salmonella* like *Salmonella enterica* subsp. *enterica* sv. Typhimurium (*S. Typhimurium*) represent a major causative agent of gastroenteritis in humans worldwide [1, 2]. Infection usually occurs through the ingestion of contaminated food or drinking water. *Salmonella* colonizes the distal small intestine, penetrates the intestinal epithelium and induces a strong inflammatory tissue response provoking the main clinical symptoms such as abdominal pain and diarrhea. In the healthy human host, non-typhoidal *Salmonella* remain restricted to the intestinal tissue. In contrast, spread to systemic organs associated with high mortality is observed in immunosuppressed individuals and newborns. This renders *Salmonella* one of the most important causative agents of neonatal sepsis and meningitis in parts of Asia and sub-Saharan Africa [3, 4]

Salmonella employs a multitude of virulence factors to overcome the mucosal barrier and evade the cellular and humoral host defence [5]. Effector molecules secreted by the *Salmonella* pathogenicity island (SPI)1-type 3 secretion system (T3SS) act during the early phase of infection and enable *Salmonella* to penetrate the intact intestinal epithelial barrier and reach the subepithelial tissue [6, 7]. SPI1-T3SS effector molecules such as SipA, SopA, SopB, and SopE₂ intimately interact with host cell processes and manipulate cellular functions such as F-actin dynamics, signal transduction, chemokine secretion, fluid homeostasis, membrane trafficking and tight junction formation [6, 8–24]. Thereby, they facilitate enterocyte invasion followed by intraepithelial proliferation, histological hallmark of *Salmonella* pathogenesis [7, 25–29]. An intact SPI1-T3SS has been strongly associated with mucosal inflammation and diarrhea and thus the clinical symptoms of *Salmonella* gastrointestinal infection in different models [30–36]. The presence in all *Salmonella* subspecies and clinical isolates indicates a critical and non-redundant function of SPI1 also during human infection [37, 38].

The functional relevance of the SPI1-T3SS for tissue infiltration, mucosal inflammation and enhanced fluid secretion *in vivo* has first been characterized using the bovine ileal loop or oral calf infection model [13, 32–34, 39–42]. Infection of calves mimics the disease in humans, characterized by small intestinal mucosal inflammation with chemokine secretion and leukocyte infiltration as well as enhanced fluid secretion [43–45]. Epithelial invasion has also been observed in guinea pig, swine and rabbit intestinal tissue [25–27, 46, 47]. In the most widely used animal model of adult mice, however, oral administration of *Salmonella* does not lead to detectable epithelial invasion and mucosal inflammation but causes a typhoid fever-like systemic infection following a largely SPI1-independent M cell-mediated mucosal translocation [48–50]. Streptomycin administration prior to infection facilitates bacterial expansion and leads to mucosal inflammation [35]. *Salmonella*-induced tissue pathology, however, is largely restricted to the caecum and colon and SPI1-dependent epithelial invasion is observed at low frequency due to rapid enterocyte exfoliation [28, 29, 35, 51, 52]. Although enterocyte invasion and intracellular proliferation has been observed in epithelial cells of the caecum of *S. Typhimurium* infected adult animals and mechanisms of host defence have been investigated [29, 53], the role of individual SPI1-T3SS mediated effector molecules during the early steps of *Salmonella* infection *in vivo* has remained ill-defined.

We have recently introduced a novel oral *Salmonella* infection model using neonate mice [50]. In this model, *Salmonella* invades the neonatal small intestinal epithelium, forms intraepithelial microcolonies and spreads to systemic organs in a strongly SPI1-T3SS dependent manner.

Here, we used this model and employed wild type *Salmonella*, *sopABE₂sipA* quadruple mutants complemented with individual effector molecules, the respective triple mutants, *sopE₂sipA*, *sopAE₂*, and *sopBE₂* double mutants as well as *sipA*, *sopB*, and *sopE₂* single mutants in combination with wild type and myeloid differentiation primary response gene 88 (MyD88)^{-/-} mice to investigate the contribution of individual SPI1-T3SS effector molecules and host factors during epithelial cell invasion and intraepithelial microcolony formation *in vivo*.

Results

Comparative analysis of individual SPI1-T3SS effector molecules by complementation

We initially employed a previously established approach using a *sopABE₂sipA* quadruple mutant *S. Typhimurium* strain complemented *in trans* by an expression plasmid encoding the respective SPI1 virulence factors SipA, SopA, SopB or SopE₂ [42]. Consistent with our previous results obtained using the SPI1-T3SS defective *S. Typhimurium invC* mutant, the *sopABE₂sipA* quadruple mutant was unable to invade murine enterocytes, failed to induce a significant transcriptional epithelial response and remained restricted to the gut lumen (S1A–S1F Fig) [50]. Complementation with *SipA* alone significantly enhanced *S. Typhimurium* viable counts in isolated enterocytes, spleen, liver and mesenteric lymph node (MLN) tissue and induced transcriptional epithelial activation (S1A–S1F Fig). Consistently, immunostaining visualized *sipA* complemented Δ *sopABE₂sipA* *Salmonella* within intestinal epithelial cells (S1G Fig). Also *sopE₂* complemented quadruple mutant *Salmonella* were observed intracellularly (S1G Fig). In contrast, no enterocyte invasion could be observed for *sopA* or *sopB* complemented Δ *sopABE₂sipA* *Salmonella* (S1G Fig). Whereas SopE₂ is conserved in all pathogenic strains of *Salmonella*, some strains additionally harbor a homologue broad-spectrum guanine nucleotide exchange factor, SopE [54–56]. Also SopE enhanced the invasive behavior leading to a significant increase in enterocyte invasion, transcriptional stimulation as well as spread to systemic tissues (S2A–S2F Fig) [57]. Importantly, albeit able to invade the epithelium, *sipA*, *sopE₂* and *sopE* complemented Δ *sopABE₂sipA* *Salmonella* were unable to proliferate and generate intraepithelial microcolonies (S1G Fig, S2G Fig).

Analysis of enterocyte invasion using triple mutants

To overcome the technical obstacles associated with *trans*-complementation such as plasmid loss, multiple effector gene copies or an impaired access of regulatory elements we next employed triple mutants leaving the fourth SPI1-T3SS effector gene under the native regulatory control. In accordance with our previous results, *sopABE₂* and *sopABsipA* mutant *Salmonella* expressing solely a functional SipA and SopE₂ effector, respectively, displayed the ability to invade primary enterocytes and enhance *Cxcl2* and *Cxcl5* mRNA expression in the intestinal epithelium (Fig 1A and 1C, S3C Fig). Both mutants also penetrated the mucosal barrier reaching liver, MLN, and spleen tissue at numbers comparable to wild type bacteria (Fig 1B, S3A and S3B Fig). In contrast, *sopBE₂sipA* and *sopAE₂sipA* mutant bacteria expressing *sopA* or *sopB* alone failed to significantly invade and penetrate the epithelium, stimulate a transcriptional response and spread to systemic organs (Fig 1A–1C). Consistently, immunostaining identified intraepithelial *Salmonella* in the presence of SipA or SopE₂ but not SopA or SopB (Fig 1D). Again, despite the intraepithelial localization, SipA expressing Δ *sopABE₂* or SopE₂ expressing Δ *sopABsipA* *Salmonella* failed to proliferate intracellularly.

Following internalization, *Salmonella* manipulates maturation of the endosomal compartment. This recruits the lysosomal-associated membrane protein (LAMP)1 from Golgi-derived

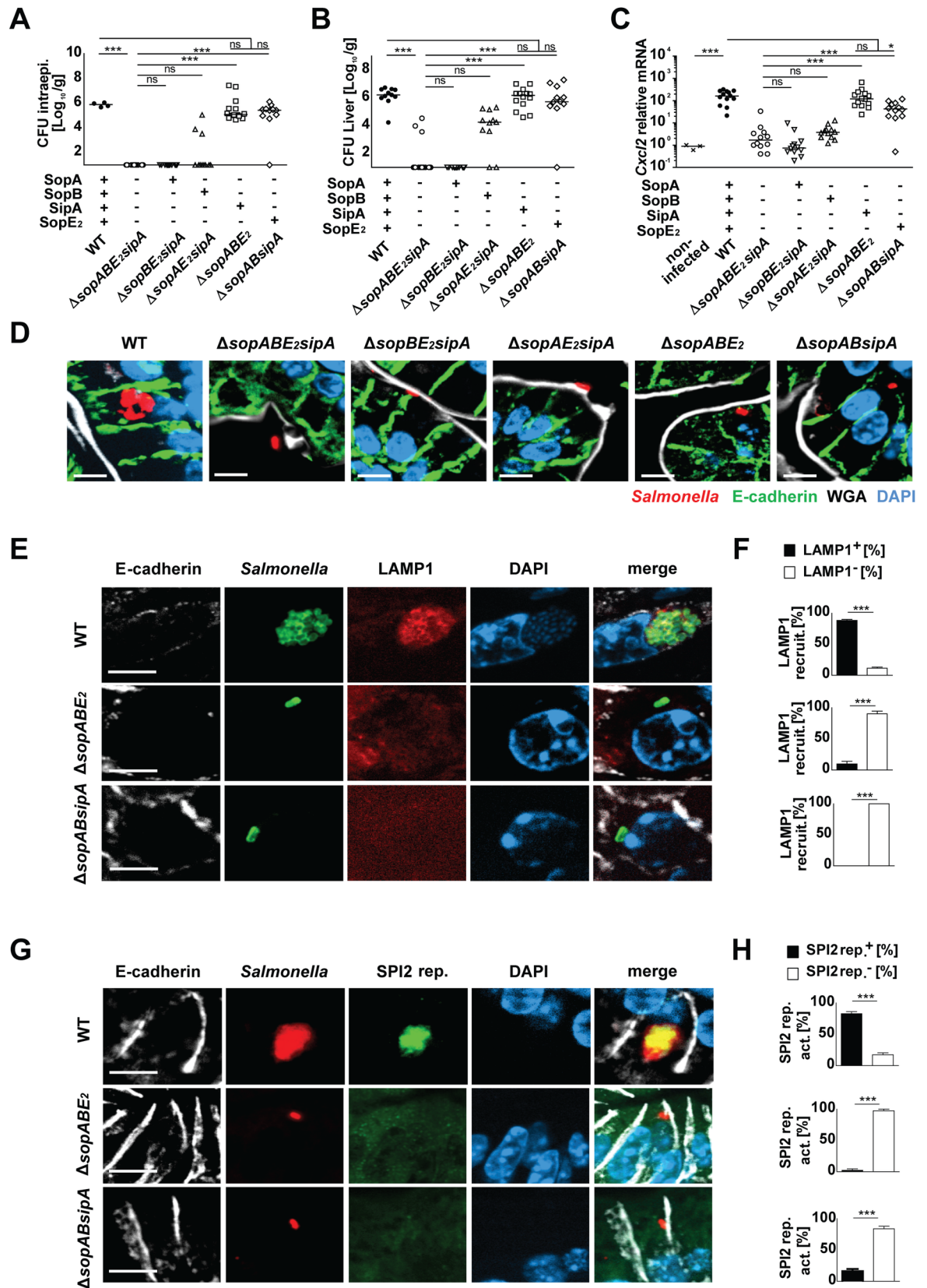


Fig 1. Comparative analysis of the role of SPI1-T3SS effector molecules SopA, SopB, SipA, and SopE₂ using triple mutants. 1-day-old C57BL/6 mice were orally infected with 100 CFU wild type (WT) (filled circles), isogenic quadruple *sopABE₂sipA* mutant (open circles), or *ΔsopBE₂sipA* (open inverted triangles), *ΔsopAE₂sipA* (open triangles), *ΔsopABE₂* (open squares), or *ΔsopABsipA* (open diamonds) *S. Typhimurium*. Viable counts in (A) isolated gentamicin-treated enterocytes and (B) total liver tissue homogenate at 4 days post infection (p.i.). (C) Quantitative RT-PCR for *Cxcl2* mRNA in total RNA prepared from enterocytes isolated at 4 days p.i.. Values were normalized to uninfected age-matched control animals (crosses). Individual values and the mean from at least two independent experiments are shown (n = 4–6 animals per group). (D) Immunostaining for *Salmonella* (red) in small intestinal tissue sections at 4 days p.i. with 100 CFU WT *S. Typhimurium* (WT), *ΔsopABE₂sipA* quadruple mutant, or *ΔsopBE₂sipA*, *ΔsopAE₂sipA*, *ΔsopABE₂*, or *ΔsopABsipA* triple mutant bacteria. Counterstaining with E-cadherin (green), WGA (white) and DAPI (blue). Bar, 5 μm. (E) Co-immunostaining for *Salmonella* WT, *ΔsopABE₂*, or *ΔsopABsipA* (green) and LAMP1 (red) in small intestinal tissue sections at day 4 p.i.. Counterstaining with E-cadherin (white) and DAPI (blue). Bar, 5 μm. (F) Quantitative evaluation of the percentage of intraepithelial *S. Typhimurium* associated with LAMP1 staining. Three tissue sections per infected neonate (n = 3) were analyzed at day 4 p.i.. Results represent the mean ± SD. (G) Co-immunostaining for *Salmonella* WT, *ΔsopABE₂* or *ΔsopABsipA* (red) and the GFP-expressing SPI2 reporter (pM973; green) in small intestinal tissue sections at day 4 p.i.. Counterstaining with E-cadherin (white) and DAPI (blue). Bar, 5 μm. (H) Quantitative analysis of the percentage of intraepithelial *S. Typhimurium* expressing the SPI2 reporter. All microcolonies from three tissue sections per infected neonate were analyzed (n = 3) at day 4 p.i.. Results represent the mean ± SD.

<https://doi.org/10.1371/journal.ppat.1006925.g001>

vesicles [58] and provides the environmental signals that coordinate the expression of SPI2-T3SS effector genes and the development of a replicative compartment [59, 60]. LAMP1 recruitment to intraepithelial bacteria was observed following infection with wild type but not *ΔsopABE₂* or *ΔsopABsipA* *Salmonella* (Fig 1E and 1F). Additionally, we used a previously described SPI2 reporter construct expressing *gfp* under the control of the *ssaG* promoter to analyze the induction of SPI2-encoded genes [52]. SPI2 reporter activity was detected in intraepithelial wild type but not SipA expressing *ΔsopABE₂* or SopE₂ expressing *ΔsopABsipA* *Salmonella* (Fig 1G and 1H).

Together, these results identified the critical but redundant role of SopE₂ and SipA for enterocyte invasion *in vivo* and highlighted the requirement of enterocyte invasion for transcriptional stimulation. Notably, invasion *per se* appeared not to be sufficient to generate an appropriate intracellular niche allowing intraepithelial bacterial proliferation. On the other hand, the formation of intraepithelial microcolonies did not significantly promote systemic spread. The ability and degree of individual SPI1-T3SS effector molecules to confer an enterocyte-invasive phenotype differed markedly between the situation *in vivo* and a classical *in vitro* cell culture-based invasion assay (S1H Fig, S2H Fig, S3D Fig) illustrating the need for a detailed investigation of the bacteria-epithelial cell interaction *in vivo* [61].

Infection-induced innate stimulation and intraepithelial proliferation

Host innate immune recognition through Toll-like receptor (TLR)2, 4 and 9 and signaling through the common adapter molecule MyD88 has previously been shown to provide the stimulatory signal for SPI2 effector gene expression and represent a prerequisite for the expression of SPI2-encoded effector genes, intracellular growth and microcolony formation in myeloid cells [60]. Interestingly, innate immune stimulation in *Salmonella*-infected neonate mice was also induced by TLR stimulation and mediated by the common adapter molecule MyD88 [50]. We therefore tested the requirement of intact MyD88-dependent signaling for intraepithelial *Salmonella* proliferation *in vivo*. As expected, MyD88-deficient mice exhibited significantly reduced epithelial *Cxcl2* and *Cxcl5* mRNA expression (S4A and S4B Fig). However, in contrast to the situation in myeloid cells, *Salmonella* maintained its ability to generate intraepithelial microcolonies with similar numbers of microcolonies per villus also in the absence of MyD88 signaling as illustrated by immunostaining and transmission electron microscopy (Fig 2A–2C). Also, LAMP1 was recruited to the majority of *Salmonella*-containing vacuole (SCV) in enterocytes and the SPI2 reporter was induced in the absence of MyD88-dependent signal transduction (Fig 2D–2G). The disease course was significantly accelerated rather than delayed, most probably as a result of an impaired MyD88-mediated antimicrobial host defence

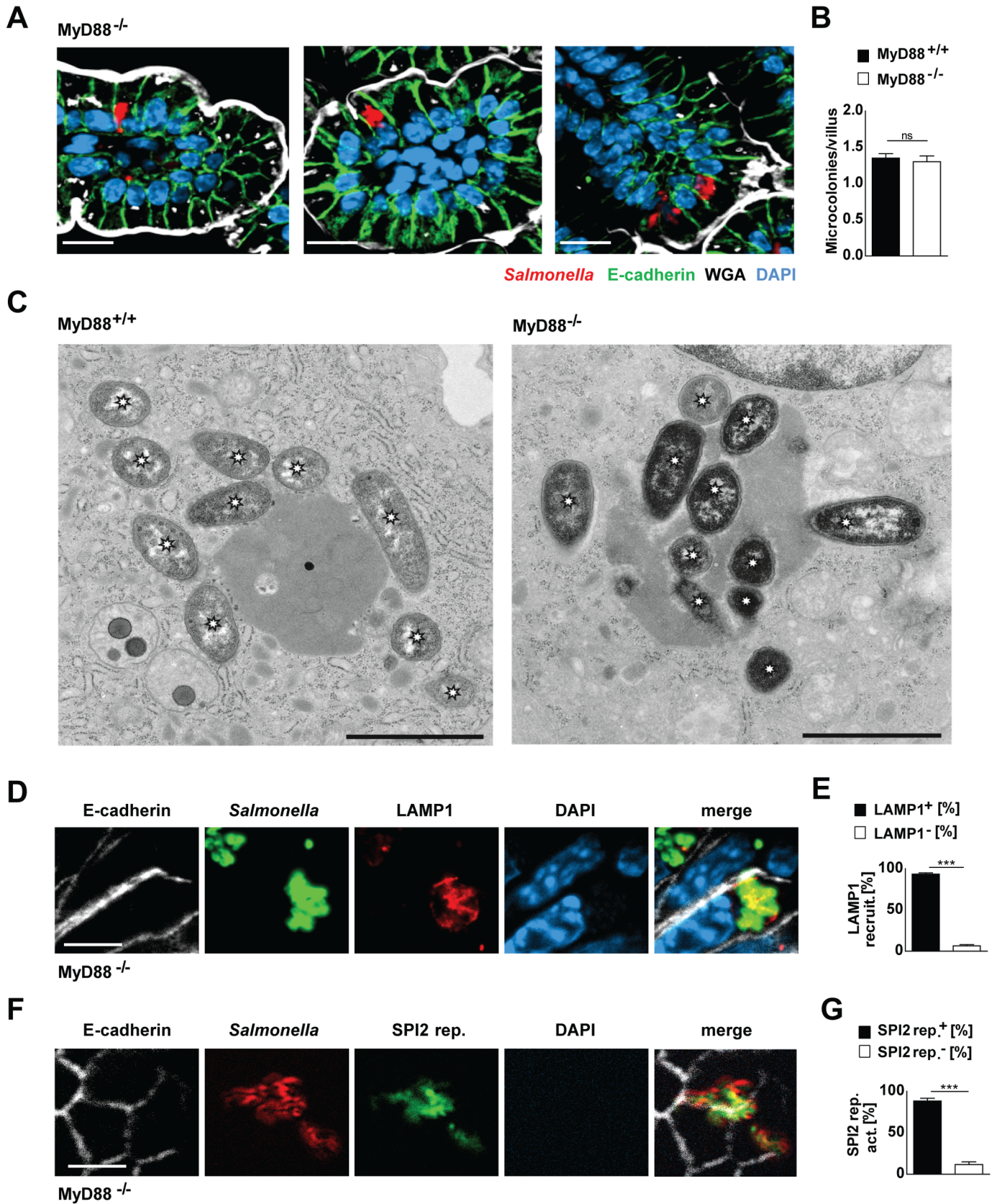


Fig 2. The influence of MyD88-dependent innate immune signaling on intraepithelial microcolony formation. 1-day-old MyD88^{+/+} and MyD88^{-/-} mice were orally infected with 100 CFU *S. Typhimurium* WT. (A) 4 days after infection, small intestinal tissues were collected and analyzed by immunostaining. Three representative images showing *S. Typhimurium* (red) forming intraepithelial microcolonies in MyD88^{-/-} mice. Counterstaining with E-cadherin (green), WGA (white) and DAPI (blue). Bar, 10 μm. For wild type controls see Fig 1D. (B) Quantitative evaluation of the number of intraepithelial microcolonies per villus in MyD88^{+/+} and MyD88^{-/-} mice at 4 days p.i.. *S. Typhimurium* microcolonies were quantified in 20–30 villi per animal (n = 6–8). Results represent the mean ± SD. (C) Transmission electron microscopy (TEM) images of intraepithelial *Salmonella* in MyD88^{+/+} (left panel) and MyD88^{-/-} mice (right panel). Asterisks highlight bacteria. Bar, 2 μm. (D) Co-immunostaining for *Salmonella* (green) and LAMP1 (red) in small intestinal tissue sections at day 4 p.i.. Counterstaining with E-cadherin (white) and DAPI (blue). Bar, 5 μm. (E) Quantitative evaluation of the percentage of intraepithelial *S. Typhimurium* associated with LAMP1 staining. Four neonates were analyzed at day 4 p.i.. Results represent the mean ± SD. (F) Co-immunostaining for *Salmonella* (red) and the GFP expressing SPI2 reporter (pM973, green) in small intestinal tissue sections at day 4 p.i.. Counterstaining with E-cadherin (white) and DAPI (blue). Bar, 5 μm. (G) Quantitative analysis of the percentage of intraepithelial *S. Typhimurium* expressing the SPI2 reporter. Microcolonies from tissue sections from four neonates were analyzed at day 4 p.i.. Results represent the mean ± SD.

<https://doi.org/10.1371/journal.ppat.1006925.g002>

(S4C Fig). Thus, intraepithelial *Salmonella* proliferation and microcolony formation occurred independently of MyD88-mediated host innate immune signaling *in vivo*.

Requirement of SPI1-T3SS effector molecules for intraepithelial microcolony formation

Although SipA or SopE₂ were sufficient to facilitate enterocyte invasion, *Salmonella* failed to induce intraepithelial microcolony formation. This suggested that intracellular proliferation required the contribution of SPI1-T3SS effector proteins beyond their invasion-promoting function. We first investigated the requirement of SipA and/or SopE₂ for intraepithelial proliferation. As expected, Δ sopE₂sipA *Salmonella* exhibited severely impaired enterocyte invasion, transcriptional stimulation and organ spread (Fig 3A–3C, S5A–S5C Fig). In contrast, sipA or sopE₂ mutant bacteria displayed only a minor phenotype with intact enterocyte invasion, transcriptional stimulation and spread to systemic organs (Fig 3D–3F, S5D–S5F Fig). Strikingly, however, sopE₂ mutant bacteria similar to wild type *Salmonella* generated LAMP1-positive intraepithelial microcolonies, whereas Δ sipA *Salmonella* failed to do so (Fig 3G, 3H and 3I). In contrast, both Δ sopE₂ and Δ sipA *Salmonella* exhibited detectable intraepithelial SPI2 reporter activity (Fig 3J and 3K). Consistent with intracellular proliferation of Δ sopE₂ *Salmonella*, the presence of SipA as compared to SopE₂ resulted in significantly higher intraepithelial viable counts (Fig 3D). The enhanced number of intraepithelial bacteria was in turn associated with increased *Cxcl2* mRNA expression as well as augmented spread to spleen, MLN and liver tissue (Fig 3E and 3F, S5D and S5E Fig).

We next defined the role of SopA and/or SopB during microcolony formation, analyzing the phenotype of sopAE₂ and sopBE₂ double mutant *Salmonella in vivo*. Both SipA expressing sopAE₂ and sopBE₂ mutants gained access to the intracellular compartment of epithelial cells, spread to systemic anatomical sites and stimulated a potent transcriptional response (Fig 4A–4C, S6A–S6C Fig). Interestingly, sopBE₂ mutant *Salmonella* failed to generate microcolonies, whereas the majority of sopAE₂ mutant-infected epithelial cells exhibited intraepithelial growth (Fig 4D and 4E). Consistently, significantly lower intraepithelial bacterial numbers were found for Δ sopBE₂ but not Δ sopAE₂ *Salmonella* as compared to wild type bacteria (Fig 4A). Also, sopAE₂ mutant but not sopBE₂ mutant *Salmonella* recruited LAMP1 (Fig 4F and 4G) and up-regulated SPI2 gene expression (Fig 4H and 4I). These results highlighted the role of SipA and SopB for intraepithelial proliferation and excluded SopA as critical SPI1 component for intraepithelial microcolony formation.

The role of SopB during the interaction of *Salmonella* with the epithelium *in vivo*

To further evaluate SopB as a potential essential effector for intraepithelial proliferation, we next tested single sopB mutant *Salmonella in vivo*. Unexpectedly, sopB mutant *Salmonella*

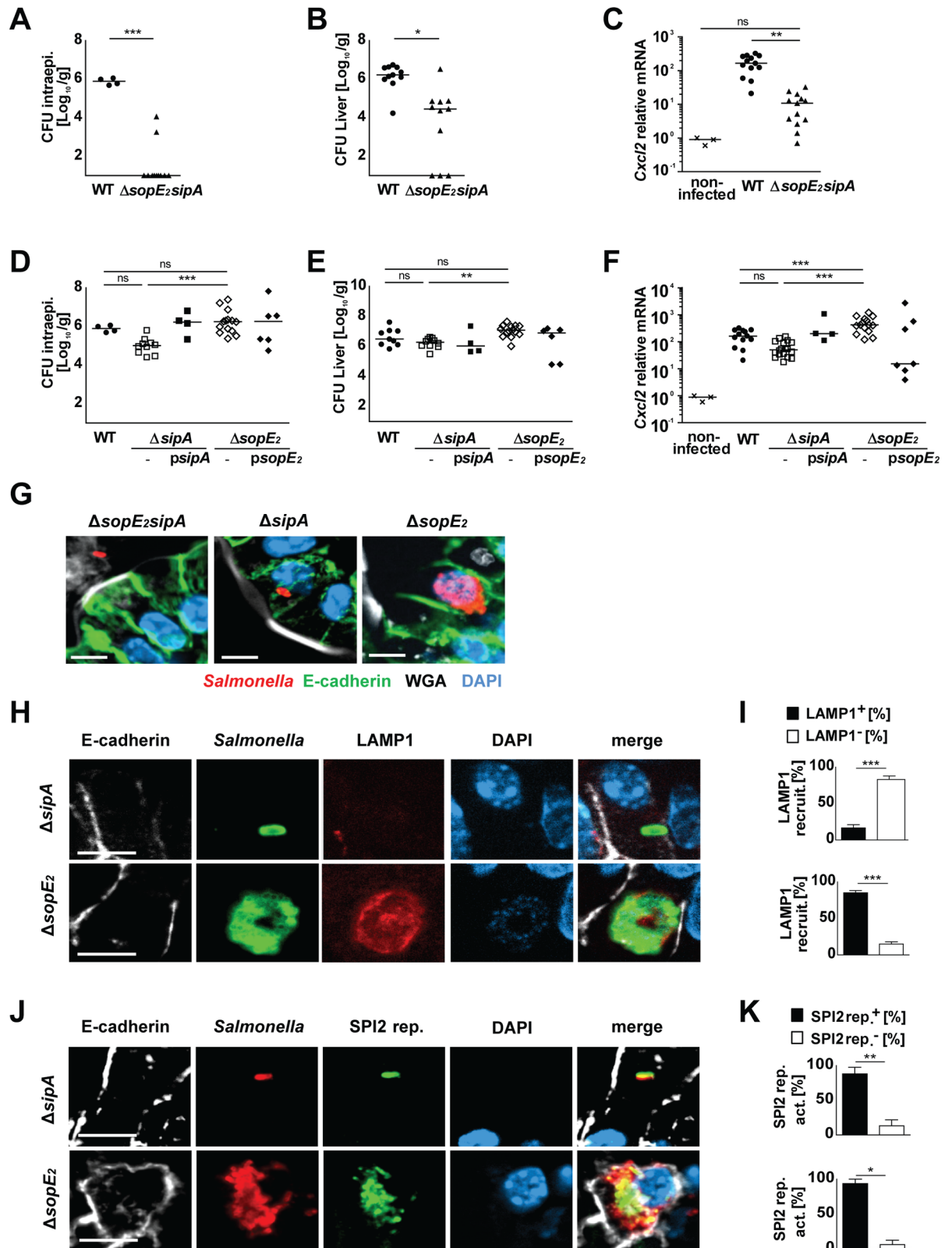


Fig 3. The redundant role of SipA and SopE₂ for enterocyte invasion. (A-C) 1-day-old C57BL/6 mice were orally infected with 100 CFU wild type (WT) (filled circles) or isogenic *sopE₂sipA* mutant *S. Typhimurium* (filled triangles). Viable counts in (A) isolated gentamicin-treated enterocytes and (B) total liver tissue homogenate at 4 days p.i.. (C) Quantitative RT-PCR for *Cxcl2* mRNA in total RNA prepared

from enterocytes isolated at 4 days p.i.. Values were normalized to uninfected age-matched control animals (crosses). Individual values and the mean from at least two independent experiments are shown ($n = 4-6$ animals per group). The data for uninfected control animals and WT *Salmonella* infected mice are identical to Fig 1A–1C. (D–F) 1-day-old C57BL/6 mice were orally infected with 100 CFU WT (filled circles), isogenic *sipA* mutant (open squares), complemented $\Delta sipA$ *psipA* (filled squares), isogenic *sopE2* mutant (open diamonds), or complemented $\Delta sopE2$ *psopE2* (filled diamonds) *Salmonella*. Viable counts in (D) isolated gentamicin-treated enterocytes and (E) total liver tissue homogenate at 4 days p.i.. (F) Quantitative RT-PCR for *Cxcl2* mRNA in total RNA prepared from enterocytes isolated at 4 days p.i.. Values were normalized to uninfected age-matched control animals (crosses). Individual values and the mean from at least two independent experiments are shown ($n = 3-5$ animals per group). The data for uninfected control animals and *Salmonella* WT infected mice are identical to Fig 1A–1C. (G) Immunostaining for *S. Typhimurium* (red) in small intestinal tissue sections at 4 days p.i. with 100 CFU $\Delta sopE2$ *sipA*, $\Delta sipA$, or $\Delta sopE2$ *S. Typhimurium* *Salmonella*. Counterstaining with E-cadherin (green), WGA (white) and DAPI (blue). Bar, 5 μ m. (H) Co-immunostaining for *Salmonella* $\Delta sipA$, $\Delta sopE2$ (green) and LAMP1 (red) in small intestinal tissue sections at day 4 p.i.. Counterstaining with E-cadherin (white) and DAPI (blue). Bar, 5 μ m. (I) Quantitative evaluation of the percentage of intraepithelial *S. Typhimurium* associated with LAMP1 staining. All microcolonies from three tissue sections per infected neonate were analyzed ($n = 5$) at day 4 p.i.. Results represent the mean \pm SD. (J) Co-immunostaining for *Salmonella* $\Delta sipA$ or $\Delta sopE2$ (red) and the GFP-expressing SPI2 reporter (pM973; green) in small intestinal tissue sections at day 4 p.i.. Counterstaining with E-cadherin (white) and DAPI (blue). Bar, 5 μ m. (K) Quantitative analysis of the percentage of intraepithelial *S. Typhimurium* expressing the SPI2 reporter. All microcolonies from three tissue sections per infected neonate were analyzed ($n = 3$) at day 4 p.i.. Results represent the mean \pm SD.

<https://doi.org/10.1371/journal.ppat.1006925.g003>

induced a more severe clinical phenotype with accelerated disease progression. Due to the accelerated disease course induced by $\Delta sopB$ *Salmonella*, the following analyses were performed at day 2 and 3 postinfection (p.i.) (Fig 5, S7 Fig). Enterocyte invasion of both wild type and $\Delta sopB$ *Salmonella* already occurred at this early time point, but spread to spleen and liver tissue remained low (Fig 5A and 5C, S7A Fig). Infection with $\Delta sopB$ *Salmonella* was accompanied by significantly enhanced *Cxcl2* and *Cxcl5* mRNA expression that was not observed during infection with wild type *Salmonella* (Fig 5D, S7B Fig). This increase in epithelial immunostimulation was associated with a significantly accelerated bacterial spread to the MLN (Fig 5B) and enhanced numbers of caspase 3- and caspase 8-positive enterocytes (Fig 5E and 5F, S7C Fig). Since a similar phenotype was not observed after infection with *sopBE2* mutant *Salmonella* (Fig 4), these results suggested that SopB by a hitherto unidentified mechanism counteracts the proapoptotic activity induced by *SopE2* [62, 63].

Strikingly, immunostaining revealed that *Salmonella* deficient solely for *sopB* were still able to proliferate intraepithelially demonstrating that SopB is not essential for intraepithelial microcolony formation (Fig 5G). Consistently, $\Delta sopB$ *Salmonella* generated LAMP1-positive intraepithelial endosomal compartments (Fig 5H and 5I) and showed induction of SPI2 reporter gene activity (Fig 5J and 5K). The fact that both *sopE2* and *sopB* single mutant *Salmonella* were able to grow intraepithelially (Figs 3G and 5G), whereas *sopBE2* double mutant *Salmonella* failed to form intraepithelial microcolonies (Fig 4D and 4E) suggests that *SopE2* and SopB exert a critical but redundant role during intraepithelial proliferation and microcolony formation.

The contribution of SipA to mucosal inflammation and intraepithelial proliferation

Neonate mice infected with the SipA-expressing *sopABE2* triple mutant *Salmonella* exhibited a more severe disease phenotype. Whereas mice infected with wild type *Salmonella* showed low but still significant weight gain during the first days after infection, mice infected with *sopABE2* mutant *Salmonella* failed to increase their body weight and exhibited an aggravated course of the disease (S8A and S8B Fig). We therefore infected 4-day-old mice in some experiments to facilitate the analysis. The accelerated disease course of $\Delta sopABE2$ *Salmonella* was associated with an increased tissue inflammation and epithelial barrier impairment illustrated by an enhanced translocation of labelled 4 kDa dextran at day 3 p.i. and a reduced length of the small intestine (Fig 6A, S8C and S8D Fig). Flow cytometric analysis of lamina propria immune cells confirmed a significantly stronger recruitment of monocytes and polymorphonuclear cells

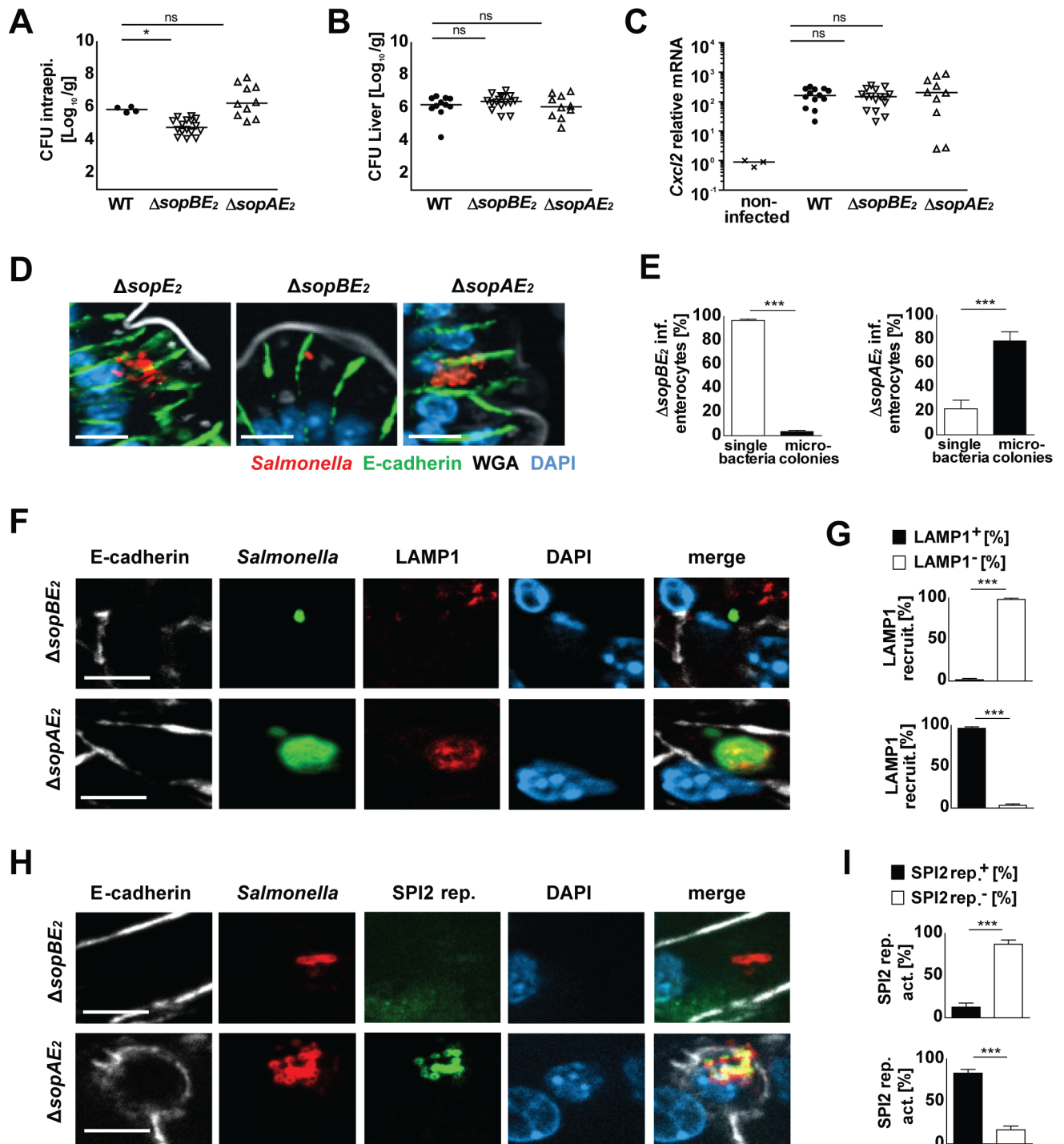


Fig 4. Analysis of *sopBE*₂ and *sopAE*₂ double mutant *S. Typhimurium*. (A–C) 1-day-old C57BL/6 mice were orally infected with 100 CFU wild type (WT) (filled circles), isogenic ΔsopBE_2 (inverted open triangles), or ΔsopAE_2 (open triangles) *S. Typhimurium*. Viable counts in (A) isolated gentamicin-treated enterocytes and (B) total liver tissue homogenate at 4 days p.i. (C) Quantitative RT-PCR for *Cxcl2* mRNA in total RNA prepared from enterocytes isolated at 4 days p.i. Values were normalized to uninfected age-matched control animals (crosses). Individual values and the mean from at least two independent experiments are shown (n = 3–6 animals per group). The data for uninfected control animals and *Salmonella* WT infected mice are identical to Fig 1A–1C. (D) Immunostaining for *Salmonella* (red) in small intestinal tissue sections at 4 days p.i. with 100 CFU ΔsopE_2 , ΔsopBE_2 , or ΔsopAE_2 *S. Typhimurium*. Counterstaining with E-cadherin (green), WGA (white) and DAPI (blue). Bar, 5 μm . (E) Percentage of epithelial cells positive for single bacteria or microcolonies (>1 intraepithelial bacterium) at 4 days p.i. with ΔsopBE_2 or ΔsopAE_2 *S. Typhimurium*. 30 *Salmonella*-positive epithelial cells per infected neonate (n = 8–13) were analyzed. Results represent the mean \pm SD. (F) Co-immunostaining for *Salmonella* ΔsopBE_2 and ΔsopAE_2 (green) and LAMP1 (red) in small intestinal tissue sections at day 4 p.i.. Counterstaining with E-cadherin (white) and DAPI (blue). Bar, 5 μm . (G) Quantitative

evaluation of the percentage of intraepithelial Δ sopBE₂ and Δ sopAE₂ *S. Typhimurium* associated with LAMP1 staining. All microcolonies from three tissue sections per infected neonate were analyzed (n = 3–4) at day 4 p.i.. Results represent the mean \pm SD. (H) Co-immunostaining for Δ sopBE₂ and Δ sopAE₂ *Salmonella* (red) and the GFP-expressing SPI2 reporter (pM973; green) in small intestinal tissue sections at day 4 p.i.. Counterstaining with E-cadherin (white) and DAPI (blue). Bar, 5 μ m. (I) Quantitative analysis of the percentage of intraepithelial *S. Typhimurium* expressing the SPI2 reporter. All microcolonies from three tissue sections per infected neonate were analyzed (n = 3–4) at day 4 p.i.. Results represent the mean \pm SD.

<https://doi.org/10.1371/journal.ppat.1006925.g004>

(PMN) 3 days after infection with Δ sopABE₂ *Salmonella* as compared to wild type *Salmonella* (Fig 6B and 6C, S8E and S8F Fig). Immunohistological detection of infiltrating PMNs corroborated the role of SipA in tissue inflammation. *Salmonella* infection enhanced the number of lamina propria PMNs and this effect was significantly reduced after infection with Δ sipA *S. Typhimurium* (S8G and S8H Fig). Notably, genetic complementation with wild type sipA (Δ sipA psipA) as well as a form of SipA with a point mutation at position 434 (Δ sipA psipA^{D434A}) previously described to harbor reduced inflammatory activity reversed this phenotype (S8G and S8H Fig). These results demonstrate an intrinsic proinflammatory activity of SipA. They are consistent with previous studies showing that SipA inhibits the phospholipid glutathione peroxidase (GPX4) and leads to enhanced secretion of the proinflammatory chemotactic eicosanoid hepxillin A₃ (HXA₃) [64, 65]. However, our results fail to confirm a significant importance of the caspase 3 cleavage site in SipA for this activity [12, 66].

The proinflammatory activity of SipA was reported to occur independently of enterocyte invasion, following secretion and binding of SipA to the epithelial surface molecule p53-effector related to PMP-22 (PERP) [12, 65, 67, 68]. Consistently, the aggravated disease phenotype was also observed after infection with *Salmonella* that lack SopA, SopB and SopE₂ and carry two point mutations in SipA (SipA^{K635A E637W}) previously shown to impair the actin-modulating activity and reduce the invasion-promoting effect of SipA (S8B Fig). The reduced invasion-promoting activity of SipA^{K635A E637W} as compared to wild type SipA was confirmed by quantification of the number of intraepithelial bacteria 2 days after infection with Δ sipA *S. Typhimurium* complemented with either psipA or psipA^{K635A E637W} (S8I Fig). The invasion-independent activity of SipA suggested that it might act *in trans* and stimulate the epithelium at anatomical locations distant to the site of enterocyte invasion.

To test whether the SipA-mediated immune stimulation contributes to the intraepithelial growth and microcolony formation, we next infected mice with a 1:1 mixture of SipA-sufficient wild type *Salmonella* and SipA-deficient Δ sopABsipA *Salmonella*. As shown in previous experiments (Fig 1A and 1D), Δ sopABsipA *Salmonella* were able to invade epithelial cells through the activity of SopE₂ but failed to proliferate intraepithelially. Following double infection, wild type *Salmonella* readily formed microcolonies in intestinal epithelial cells (Fig 6D, double stained appearing in yellow). In contrast, Δ sopABsipA *Salmonella* invaded but failed to proliferate intracellularly (Fig 6D, in red). Thus, the induction of a proinflammatory signal by SipA-expressing wild type *Salmonella* was not sufficient to induce a replicative endosomal environment in distant enterocytes and rescue the intraepithelial proliferation defect of SipA-deficient Δ sopABsipA *Salmonella*.

Next, we investigated the intrinsic activity of SipA *in vivo*. We therefore analyzed Δ sipA *Salmonella* complemented *in trans* with the gene for (i) wild type SipA (Δ sipA psipA) (ii) SipA with two point mutations at position 635 and 637 previously shown to impair its actin stabilization and reduce the invasion-promoting activity (Δ sipA psipA^{K635A E637W}) [67] (S8I Fig), (iii) SipA that lacks the caspase 3 cleavage site reported to be critical for the proinflammatory activity [66] (Δ sipA psipA^{D434A}) and (iv) SipA that lacks both, the actin-stabilizing and proinflammatory activity (Δ sipA psipA^{D434A K635A E637W}). Expression of these constructs was tested in the presence of SopE₂ to ensure enterocyte invasion and allow the comparative analysis of the different SipA variants in respect to intraepithelial growth and microcolony formation. As

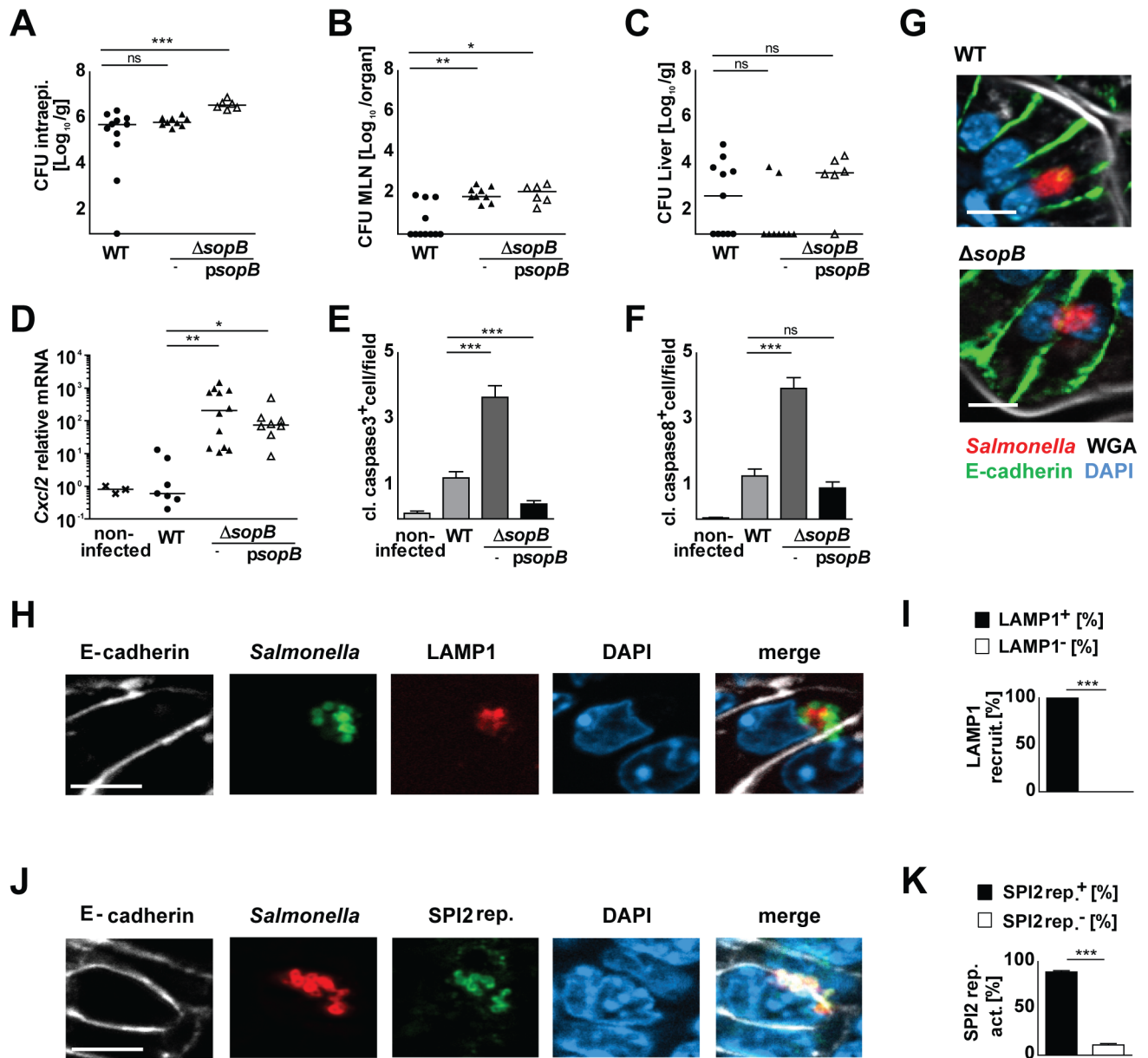


Fig 5. The role of SopB in the interaction between *Salmonella* and the epithelium. 1-day-old C57BL/6 mice were orally infected with 100 CFU wild type (WT) (filled circles), isogenic *sopB* mutant (filled triangles), or *psopB*-complemented ΔsopB (open triangles) *S. Typhimurium*. Viable counts in (A) isolated gentamicin-treated enterocytes, (B) total MLN and (C) total liver tissue homogenate at 2 days p.i.. (D) Quantitative RT-PCR for *Cxcl2* mRNA in total RNA prepared from enterocytes isolated at 2 days p.i.. Values were normalized to uninfected age-matched control animals (crosses). Individual values and the mean from at least two independent experiments are shown ($n = 3-5$ animals per group). (E) Quantitative analysis of the number of cleaved caspase 3- and (F) cleaved caspase 8 positive cells per 200 times magnification image field. Positive cells from 20 image fields from one section were analyzed per infected neonate ($n = 3-6$) at day 3 p.i.. Results represent the mean \pm SD. (G) Immunostaining for *S. Typhimurium* (red) in small intestinal tissue sections at 3 days p.i. with 100 CFU WT and ΔsopB *S. Typhimurium*. Counterstaining with E-cadherin (green), WGA (white) and DAPI (blue). Bar, 5 μm . (H) Co-immunostaining for ΔsopB *S. Typhimurium* (green) and LAMP1 (red) in small intestinal tissue sections at day 3 p.i.. Counterstaining with E-cadherin (white) and DAPI (blue). Bar, 5 μm . (I) Quantitative evaluation of the percentage of intraepithelial *S. Typhimurium* associated with LAMP1 staining. All microcolonies from three tissue sections per infected neonate were analyzed ($n = 3$) at day 3 p.i.. Results represent the mean \pm SD. (J) Co-immunostaining for ΔsopB *S. Typhimurium* (red) and the GFP expressing SPI2 reporter (pM973; green) in small intestinal tissue sections at day 3 p.i.. Counterstaining with E-cadherin (white) and DAPI (blue). Bar, 5 μm . (K) Quantitative analysis of the percentage of intraepithelial *S. Typhimurium* expressing the SPI2 reporter. All microcolonies from three tissue sections per infected neonate were analyzed ($n = 3$) at day 3 p.i.. Results represent the mean \pm SD.

<https://doi.org/10.1371/journal.ppat.1006925.g005>

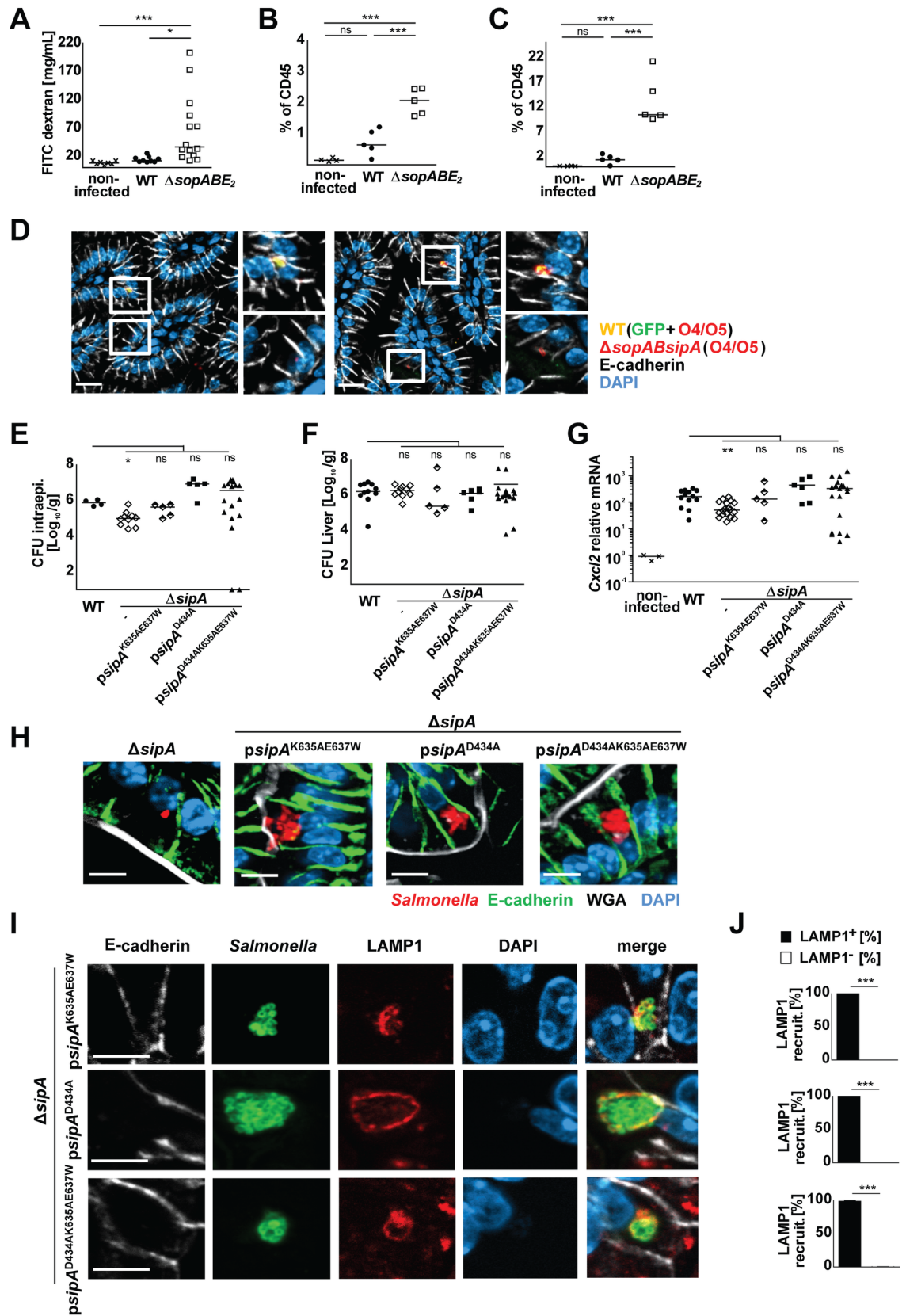


Fig 6. The role of SipA for intraepithelial microcolony formation. (A) Mucosal barrier integrity tested by serum quantification 4 hours after oral administration of FITC labeled-4kDa dextran. 1-day-old C57BL/6 mice were left untreated (crosses) or infected with WT (filled circles) or Δ sopABE₂ (open squares) *S. Typhimurium*. FITC labeled-4 kDa dextran was quantified in serum at day 3 p.i. as indicated. (B and C) Flow cytometric analysis of lamina propria immune cells. 4-day-old mice were left untreated or orally infected with 100 CFU WT or Δ sopABE₂ *S. Typhimurium* and total small intestinal leukocytes were analyzed by flow cytometry at day 3 p.i.. (B) Monocytes (Ly6C^{hi}Ly6G^{CD11b}⁺ MHCII^{lo/-} CD45⁺ DAPI) and (C) neutrophils (Ly6G⁺Ly6C^{int}CD11b⁺ MHCII^{lo/-} CD45⁺ DAPI) are depicted as percentage of CD45⁺ cells in non-infected (crosses), WT (filled circles) and Δ sopABE₂ *Salmonella* (open squares). The results represent the mean values from at least two independent experiments (n = 4–6 per group). (D) Immunostaining for *Salmonella* in small intestinal tissue sections at 4 days after co-infection with 100 CFU GFP-expressing WT (yellow) and *SopABsipA* (red) *S. Typhimurium*. WT *Salmonella* appear in yellow due to simultaneous staining for O4/O5 antigen (red) and GFP (green). *SopABsipA Salmonella* appear in red due to simultaneous staining for O4/O5 antigen (red). Counterstaining with E-cadherin (white) and DAPI (blue). Bar, 10 μ m. (E–J) 1-day-old C57BL/6 mice were orally infected with 100 CFU WT (filled circles), Δ sipA (open diamonds), Δ sipA complemented with *psipA*^{K635A E637W} (half-filled diamonds), Δ sipA complemented with *psipA*^{D434A} (filled squares), or Δ sipA complemented with *psipA*^{D434A K635A E637W} (filled triangles) *S. Typhimurium*. Viable counts in (E) isolated gentamicin-treated enterocytes and (F) total liver tissue homogenate at 4 days p.i.. (G) Quantitative RT-PCR for *Cxcl2* mRNA in total RNA prepared from enterocytes isolated at 4 days p.i.. Values were normalized to uninfected age-matched control animals (crosses). Individual values and the mean from at least two independent experiments are shown (n = 4–7 animals per group). The data for WT *Salmonella* infected mice and uninfected control animals are identical to Fig 1A–1C. (H) Immunostaining for *Salmonella* (red) in small intestinal tissue sections at 4 days p.i. with 100 CFU Δ sipA, Δ sipA complemented with *psipA*^{K635A E637W}, Δ sipA complemented with *psipA*^{D434A}, or Δ sipA complemented with *psipA*^{D434A K635A E637W} *S. Typhimurium*. Counterstaining with E-cadherin (green), WGA (white) and DAPI (blue). Bar, 5 μ m. (I) Co-immunostaining for LAMP1 (red) and Δ sipA complemented with *psipA*^{K635A E637W}, Δ sipA complemented with *psipA*^{D434A}, or Δ sipA complemented with *psipA*^{D434A K635A E637W} *S. Typhimurium* (green) in small intestinal tissue sections at day 4 p.i.. Counterstaining with E-cadherin (white) and DAPI (blue). Bar, 5 μ m. (J) Quantitative evaluation of the percentage of intraepithelial *S. Typhimurium* associated with LAMP1 staining. All microcolonies from three tissue sections per infected neonate were analyzed (n = 3) at day 4 p.i.. Results represent the mean \pm SD.

<https://doi.org/10.1371/journal.ppat.1006925.g006>

expected, Δ sipA, Δ sipA *psipA*^{K635A E637W}, Δ sipA *psipA*^{D434A} and Δ sipA *psipA*^{D434A K635A E637W} *Salmonella* were able to invade the epithelium (Fig 6E), cause systemic infection (Fig 6F, S9A and S9B Fig) and induce transcriptional stimulation (Fig 6G, S9C Fig). As observed before, Δ sipA *Salmonella* exhibited significantly reduced intraepithelial bacterial numbers and *Cxcl2* mRNA expression, and failed to proliferate and form intraepithelial microcolonies (Fig 6E, 6G and 6H). Infection with Δ sipA *Salmonella* was also associated with a moderately reduced mortality (S9D Fig). In contrast, Δ sipA *Salmonella* complemented with *psipA*^{K635A E637W}, *psipA*^{D434A}, *psipA*^{D434A K635A E637W} behaved indistinguishably from wild type *Salmonella* and readily formed LAMP1-positive intraepithelial microcolonies (Fig 6I and 6J). Together, these results demonstrate the critical importance of SipA. However, in the presence of SopE₂, neither the actin-stabilizing activity nor the reported caspase 3-dependent proinflammatory activity were required for intraepithelial proliferation and microcolony formation.

Discussion

Salmonella expressing SopE, SopE₂ or SipA but not Δ sopE₂sipA *Salmonella* were able to invade the epithelium indicating that the production of SopE, SopE₂ or SipA is necessary and sufficient to facilitate enterocyte invasion *in vivo*. SopE or SopE₂ activate the Rho GTPases Rac-1 and Cdc42 or only Cdc42, respectively, leading to actin assembly, membrane ruffling and bacterial internalization [22–24, 54, 56]. SipA with its C-terminal domain stabilizes actin filaments, promoting bacterial invasion in the absence of prominent membrane ruffling [9–12, 42, 69]. Their potent activity was illustrated by the finding that the presence of only one of the two effector molecules facilitated enterocyte invasion at levels indistinguishable from wild type bacteria. Notably, also the ubiquitin E3 ligase SopA was previously shown to contribute to invasion of polarized epithelial cells *in vitro* [15, 16, 42]. Also SopB was shown to promote membrane fission and bacterial invasion [18, 19, 70, 71]. It was suggested that SopB supports SopE-mediated actin filament polymerization by recruiting ARNO (Cytohesin2) to the site of invasion [72]. Our *in vivo* results do not support a significant role for SopA or SopB in enterocyte entry. However, although unlikely, we cannot exclude that enterocyte invasion by strains

expressing effectors other than sipA or sopE₂ occurred but remained undetected due to rapid enterocyte apoptosis or exfoliation as observed in adult mice [29].

Consistent with previous *in vitro* results, enterocyte invasion was not sufficient to allow proliferation and microcolony formation despite the presence of a fully functional SPI2 locus [73]. Δ sopB, Δ sopE₂ and Δ sopAE₂ but not Δ sipA *Salmonella* were able to generate intraepithelial microcolonies assigning SipA a critical non-redundant role for intracellular growth. Δ sipA *Salmonella* failed to recruit LAMP1 to the endosomal epithelial compartment, confirming a recent report on the contribution of the NH₂-terminal domain of SipA (aa1-458) to endosomal maturation and intracellular replication [74]. SipA was recently also shown to promote intracellular proliferation via interaction with the actin nucleator family member Spire2 [69]. In our study, the SipA activity required for intraepithelial microcolony formation was independent of its actin stabilizing function or proinflammatory activity reported to depend on caspase 3 processing [66, 67]. This might be explained by the recently described cooperative action of SipA with the SPI2 effector SifA to promote phagosome maturation and the generation of a replicative intraepithelial compartment [74]. Interestingly, intraepithelial Δ sipA *Salmonella* exhibited expression of the SPI2 reporter indicating that SPI2 effector expression can occur independently of SipA.

Whereas both Δ sopE₂ and Δ sopB *Salmonella* readily proliferated in enterocytes, *sopBE*₂ mutant *Salmonella* were unable to form intraepithelial microcolonies. Consistently, Δ sopBE₂ and Δ sopABE₂ (in contrast to Δ sopE₂ or Δ sopB) *Salmonella* failed to recruit LAMP1 to the endosomal compartment and to turn on SPI2 gene expression. Thus, SopB and SopE₂ contributed in a redundant fashion to the generation of a replicative endosomal compartment in enterocytes. Both, SopE₂ and SopB activate Rho GTPases and mitogen activated protein kinases (MAPK), which might contribute to endosomal modification [22–24, 72]. Alternatively, SopB was described to directly or indirectly lead to the accumulation of phosphatidylinositol 3-phosphate on the outer leaflet of the SCV, altering the recruitment of host cell endocytic trafficking molecules and thereby preventing SCV-lysosomal fusion [17, 18, 75, 76]. Although SopE₂ was shown to influence endosomal maturation and intracellular proliferation, it is currently unknown how it could compensate for the lack of SopB [77].

Enterocyte invasion was consistently associated with a transcriptional stimulation of the intestinal epithelium. In contrast, non-invasive Δ sopABE₂sipA *Salmonella* failed to evoke a significant epithelial response despite the presence of high numbers of bacteria in the intestinal lumen. Also, the presence of a functional T3SS system in the absence of invasion in *sopAE*₂-sipA, *sopBE*₂sipA or *sopE*₂sipA mutant bacteria was unable to induce a significant epithelial transcriptional response. Whereas invasion led to a more than 100-fold increase in *Cxcl2* and *Cxcl5* mRNA expression, intraepithelial proliferation only moderately contributed to this response. Our results therefore suggest that the presence of intraepithelial *Salmonella per se* or, alternatively, downstream events such as stimulation of lamina propria immune cells as a consequence of penetration of the epithelial barrier drive epithelial transcriptional stimulation [67]. This is consistent with the previously reported requirement of a functional SPI1 system to evoke PMN transmigration and fluid secretion in calves and the bovine ligated loop model [32–34]. It is also in accordance with the presence of a functional SPI1 locus among all isolates from symptomatic human patients [37, 38].

In addition to the stimulation of pattern recognition receptors the activation of host cell signaling pathways by *Salmonella* virulence factors has been described. For example, SopA was reported to contribute to tissue inflammation by targeting two host E3 ubiquitin ligases, TRIM56 and TRIM65 [13, 15, 78]. Also SopB was shown to indirectly stimulate Rho family GTPases and nuclear responses [56]. However, no significant influence of SopA or SopB on chemokine expression was observed in our study. Instead, our results suggest that SopA

together with SopB and/or SopE₂ may contribute to balance the adverse effects of the inflammatory activity of SipA. Additionally, T3SS-mediated translocation of SipA and SopE₂ was reported to directly induce host cell activation [23, 79]. SopE-mediated activation of the Rho family of small molecular weight GTPase Cdc42 and activation of p21-activated kinase was reported to induce mitogen-activated protein (MAP) kinase and NF-κB stimulation [23, 80, 81]. However, invasive Δ sopABsipA and Δ sopABE₂ *Salmonella* (in the absence of SipA and SopE₂, respectively) still provoked potent transcriptional enterocyte stimulation *in vivo*.

SipA (SipA₂₉₄₋₄₂₄) was additionally shown to induce PMN transmigration and tissue inflammation via PKCα-dependent secretion of the chemotactic eicosanoid hepxillin A₃ (HXA₃) [12, 65, 82]. Notably, this pro-inflammatory activity was demonstrated to be independent of actin filament stabilization and enterocyte invasion and thus differed from the invasion-mediated immune stimulation discussed above [52, 65, 67, 82]. Binding of SipA to the epithelial surface molecule p53-effector related to PMP-22 (PERP) was shown to inhibit the phospholipid glutathione peroxidase (GPX4) [12, 65, 67, 68]. This effect was also observed *in vivo* with major influence on epithelial barrier integrity, immune cell infiltration and the outcome of the disease. Consistent with previous reports, immune stimulation was still observed in sipA^{K635A E637W} Δ sopABE₂ *Salmonella* despite a reduced invasiveness, supporting the idea that SipA acts extracellularly to stimulate the mucosal immune system [65, 68]. However, no influence of this SipA-mediated immune stimulation was observed on intraepithelial proliferation. The fact that Δ sopABE₂ *Salmonella* exhibited a more severe proinflammatory effect as compared to SipA-competent wild type bacteria suggests that SopA, SopB or SopE₂ might counteract this SipA effect *in vivo*.

Enhanced epithelial apoptosis and increased mortality were noted in the absence of SopB, consistent with a recent report that demonstrated protection from Nlrc4/ASC-mediated apoptosis by SopB *in vitro* [20, 83]. SopB might additionally prevent apoptosis by other mechanisms [21, 84]. Epithelial barrier damage after infection with Δ sopB *Salmonella* explains the higher bacterial load in the mesenteric lymph node. Intriguingly, enhanced disease progression following infection with Δ sopB *Salmonella* was absent using Δ sipAsopBE₂ and Δ sopBE₂ *Salmonella*. This suggests that the apoptosis-promoting effect is SopE₂-mediated. Indeed, SopE₂ has long been described to activate the c-jun NH₂-terminal kinase (JNK) [23, 80] and JNK signaling is known to drive ROS-induced caspase 3-dependent apoptosis [85]. Alternatively, SopE₂ was recently shown to activate caspase 1 [63]. Thus, our results identify a previously undescribed role for SopB: to protect from SopE₂-mediated epithelial cell damage.

Despite the lack of intraepithelial microcolonies, Δ sopABsipA, Δ sopABE₂, Δ sopBE₂ or Δ sipA *Salmonella* efficiently penetrated the epithelial barrier and spread to systemic organs, reaching levels in spleen and liver tissue comparable to wild type *Salmonella*. This suggests that intraepithelial replication, although considered a hallmark of *Salmonella* pathogenesis, does not represent a prerequisite for efficient penetration of the epithelial barrier. This is consistent with the observation by Müller et al., who described SPI1-T3SS dependent penetration of the colon epithelium in the absence of detectable intraepithelial growth [28]. We even cannot exclude that two different bacterial populations simultaneously drive mucosal translocation and systemic spread. These results indicate that the functional relevance of intraepithelial replication and SCV formation has not been fully established and warrants further investigation.

Together, we validate the new neonatal infection model and present the first detailed *in vivo* analysis of the host and bacterial factors required for enterocyte invasion and intraepithelial microcolony formation, hallmark of *Salmonella* pathogenesis (Fig 7, S3 Table). We define the redundant and cooperative function of the SPI1-T3SS effectors SopA, SopB, SopE₂ and SipA for invasion of the intestinal epithelium and intraepithelial growth and characterize their influence on innate immune stimulation, mucosal translocation and spread to systemic

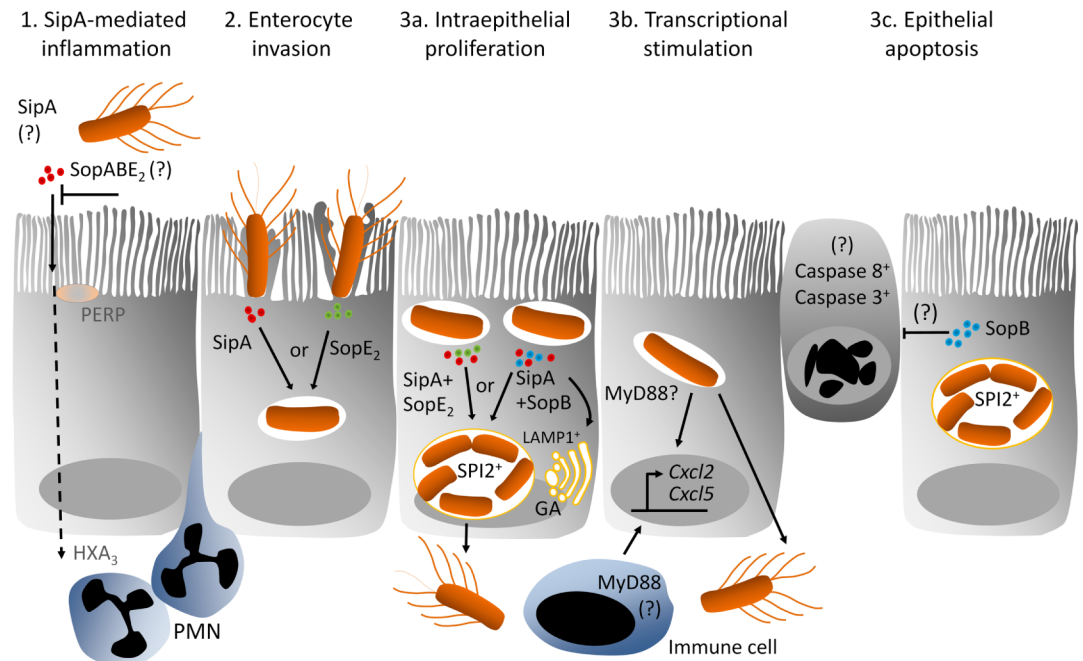


Fig 7. Graphical illustration of the role of the SPI1-T3SS effectors SopA, SopB, SopE₂ and SipA during enterocyte invasion and intraepithelial proliferation *in vivo*. (1) SipA (red dots) promotes the early recruitment of PMNs and causes barrier disruption and disease progression. This has been reported to occur via stimulation of the epithelial surface molecule p53-effector related to PMP-22 (PERP) and activation of the chemotactic eicosanoid hepxillin A₃ (HXA₃) [68, 89]. This effect appears to be invasion-independent and strongly enhanced in the absence of SopA, SopB and SopE₂ suggesting that these effectors exert regulatory functions. (2) Among the studied effector molecules, expression of SipA (red dots), SopE₂ (green dots), or SopE (not shown here) alone is sufficient to facilitate enterocyte invasion. Intraepithelial *Salmonella* then reside within a LAMP1 negative endosomal compartment and fail to proliferate or express SPI2 encoded genes. (3a) SipA together with SopE₂ or SipA together with SopB (blue dots) facilitate the recruitment of LAMP1 (yellow membrane) from the Golgi apparatus (GA) and the generation of a replicative compartment with intraepithelial bacterial proliferation and expression of SPI2 encoded genes. (3b) Enterocyte invasion or, alternatively, penetration of the epithelial barrier *via* innate stimulation and signaling through MyD88 induce expression of the chemokines *Cxcl2* and *Cxcl5* in the epithelium. (3c) SopB appears to directly or indirectly inhibit caspase 3 and caspase 8 mediated epithelial cell apoptosis. GA, golgi apparatus; HXA₃, hepxillin A₃; LAMP1, lysosomal-associated membrane protein 1; PERP, p53-effector related to PMP-22; SPI2, *Salmonella* pathogenicity island 2.

<https://doi.org/10.1371/journal.ppat.1006925.g007>

organs. Our results thereby significantly extend our insight in the early steps of the microbial-host interplay *in vivo* and might reveal new targets for future preventive and therapeutic measures.

Materials and methods

Bacterial strains and plasmids

All bacterial mutants and plasmids used in this study are listed in the [S1 Table](#). *Salmonella enterica* subsp. *enterica* serovar Typhimurium ATCC14028 were used as wild type bacteria. The *sopABE₂sipA* quadruple mutant *S. Typhimurium* carrying the low copy number pWSK29 vector encoding *sopA*, *sopB*, *sipA*, *SopE* or *sopE₂*, or the empty pWSK29 vector as control, as well as the respective isogenic *S. Typhimurium* triple, double or single mutants were used to analyze individual SPI1-T3SS effector molecules. Deletions of genes encoding effector proteins were generated by Red-mediated recombination basically as described before [86]. Strains with multiple deletions of effector genes were generated by P22-mediated transduction of mutant alleles containing the *aph* or *CAT* cassette. If required to generate multiple mutations

by Red-mediated mutagenesis, antibiotic resistance genes were removed by FLP-mediated recombination between FRT sites. For the generation of a strain with point mutations in chromosomal *sipA* a two-step scarless mutagenesis approach according to Hoffmann et al. was applied [86]. A targeting cassette from pWRG717 was amplified using sipA633 In717 For and sipA939 In717 Rev (S2 Table). *Salmonella* WT harboring pWRG730 was induced for expression of red $\alpha\beta\gamma$ and transformed to kanamycin resistance. The resulting *sipA* mutant allele was transferred to other mutant strains using P22 transduction. The mutant allele *sipA* K635A E637W was amplified by PCR from plasmid p4758 target strains and the resulted DNA was used to transform MvP2511 harboring pWRG730. Resistance to I-SceI-mediated double strand breaks was used for selection of homologous recombination basically as described by Hoffmann et al. [86]. The point mutations in resulting strain MvP2520 were confirmed by DNA sequencing. Finally, the *sopE*₂::aph mutation was introduced by P22 transduction to yield MvP2521.

For complementation of *sipA*, *sopA*, *sopB*, *sopE* or *sopE*₂ deletions, the corresponding genes were amplified from *S. enterica* sv. Typhimurium genomic DNA introducing 3' HA tag sequences for detection of the encoded proteins by immunoblotting. Oligonucleotides for amplification are listed in S2 Table. PCR products were cloned in low copy number vector pWSK29 and *E. coli* DH5 α was used to propagate plasmids p4041, p4042, p4043 and p4044, SopA::HA, SopB::HA, SopE::HA, and SopE₂::HA, respectively. Since *sipA* is the terminal gene of the *sicAsipBCDA* operon, the P_{sicA} promoter was amplified and cloned upstream of *sipA*::HA to generate p4040. Mutant strains were transformed with complementation plasmids listed in S1 Table. Synthesis and translocation of the effector proteins by *S. Typhimurium* was confirmed by immunolabelling of the HA tag. Furthermore, the plasmids gradually complemented the invasion defect of a multi-effector mutant strain. The function of SipA was additionally analyzed using Δ *sipA* *Salmonella* carrying the *sipA* gene with point mutations at specific functional positions. Vector p4758 carrying two point mutations in the *sipA* gene at the actin binding site (amino acid position 635 and 637), vector p4890 carrying a point mutation in the *sipA* gene at the caspase 3 motif (amino acid position 434), and vector p4892 carrying all three point mutations in the *sipA* gene were generated by site-directed mutagenesis. Site-directed mutagenesis was performed using the Q5 SDM kit according to the manufacturers' protocol (NEB). Multiple rounds of mutagenesis were performed if required for the generation of double or triple mutations using primers listed in the S2 Table. The plasmid with constitutive green fluorescent protein (GFP) expression (pGFP, AmpR) was kindly provided by Brendan Cormack, Stanford, USA. The reporter construct pM973 expressing *gfp* under the control of the SPI2 promoter *psaG* (AmpR) kindly provided by Wolf D. Hardt, ETH Zürich, Switzerland was used to analyze the expression of SPI2 effector molecules by intraepithelial *Salmonella*.

***In vitro* infection experiments**

Intestinal epithelial m-IC_{cl2} cells were cultured as previously described [87]. Bacteria were cultured in Luria Bertani (LB) broth at 37°C in the presence of 100 μ g/mL ampicillin, 50 μ g/mL kanamycin, or 100 μ g/mL carbenicillin. Overnight cultures were diluted 1:10 and incubated at 37°C for approximately 80 min until reaching the logarithmic phase (OD₆₀₀ approximately 0.5). Bacteria were then washed three times in PBS and the OD₆₀₀ was adjusted to 0.55–0.60 corresponding to approximately 2.0 \times 10⁸ CFU bacteria per mL. The bacterial suspension was subsequently diluted to obtain the appropriate infection dose. Bacteria were added to the m-IC_{cl2} cells (2 \times 10⁵ cells per well) at a multiplicity of infection (MOI) of 1:10. The cell culture plate was centrifuged at 300xg for 5 min and incubated at 37°C for 1 h. Cells were washed

three times with PBS and cell culture medium supplemented with 100 µg/mL gentamicin (Sigma) was added. After incubation at 37°C for 1 h, cells were washed again three times in PBS and lysed for 2 min at room temperature in 500 µL 0.1% Triton X-100 (Roth) in aqua dest. Viable bacteria were quantified by serial dilution and plating.

Ethics statement

All animal experiments were performed in compliance with the German animal protection law (TierSchG) and approved by the local animal welfare committee (Niedersächsische Landesamt für Verbraucherschutz und Lebensmittelsicherheit Oldenburg, Germany; Landesamt für Natur, Umwelt und Verbraucherschutz, North Rhine Westfalia) under the code 8402.04.2015A073, 84-02.042015.A067, 84-02.042015.A065 and 81-02.04.2017.A397 including all approved changes.

In vivo infection experiments

Adult C57BL/6J wild type and B6.129P2(SJL)-*MyD88^{tm1.1Defr}/J* (*MyD88^{-/-}*, stock no. 009088) were obtained from the Jackson Laboratory (Bar Harbour, USA) and bred locally under SPF conditions. Bacteria were cultured as described above. 1- and 4-day-old animals were orally infected with 100 CFU of wild type *S. Typhimurium* or the indicated isogenic mutants in a volume of 1 µL PBS. At various time points post infection (p.i.), liver, mesenteric lymph node (MLN) and spleen were collected and homogenized in sterile PBS. Viable counts were obtained by serial dilution and plating on LB agar plates supplemented with the appropriate antibiotics. Alternatively, small intestinal tissues were collected at the indicated time point p.i. and prepared for immunostaining or electron microscopy. For co-infection, 100 CFU of *Salmonella* wild type carrying pGFP and *sopABsipA* mutant *Salmonella* were administered orally to 1-day-old mice at a ratio of 1:1 in 2 µL.

Primary epithelial cell isolation

Primary small intestinal epithelial cells (IEC) from neonate mice were isolated as previously described [87]. Briefly, the small intestinal tissue was cut in small pieces and incubated in 30 mM EDTA/PBS at 37°C for 10 min. IEC were detached from the underlying tissue by shaking. Cells were then filtered through a 100 µm nylon cell strainer (BD Falcon) and harvested by centrifugation at 300xg for 10 min. The cell pellet was resuspended in 10% FCS/PBS and harvested by centrifugation at 300xg for 10 min. To obtain the intraepithelial bacterial count, IEC were treated with 100 µg/mL gentamicin for 1 h at room temperature as previously described and subsequently lysed and plated in serial dilutions on selective LB agar plates [50].

Gene expression analysis

Total RNA was extracted from isolated IEC using TRIzol (Invitrogen) and the RNA concentration was determined on a NanoDrop 1000 spectrophotometer (Thermo Scientific). First-strand complementary DNA (cDNA) was synthesized from 5 µg total RNA using Oligo-dT primers, RevertAid reverse transcriptase and RiboLock RNase inhibitor (ThermoFisher Scientific). RT-PCR was performed using the Taqman technology with an absolute QPCR ROX mix (Thermo Scientific), sample cDNA and the Taqman probes *Hprt* (Mm00446968-m1), *Cxcl2* (Mm00436450_m1) and *Cxcl5* (Mm00436451_g1) (Life Technologies). Results were calculated by the $\Delta\Delta$ -CT method. For data analysis, values were normalized to the *hprt* housekeeping gene and were presented as fold induction over age-matched controls.

FITC dextran-mediated analysis of epithelial barrier function

Infected mice were orally administered 2 μ L of a 0.6 mg/ μ L 4kDa FITC dextran solution (TdB Consultancy) at the indicated time point p.i.. After four hours, serum was collected and the serum concentration of FITC dextran was measured by fluorometry using a SpectraMax i3 at an excitation of 492nm (9 nm bandwidth) and an emission of 518nm (15 nm bandwidth) using a serially diluted FITC dextran solution as standard.

Immunofluorescence staining

4 μ m paraformaldehyde-fixed paraffin-embedded tissue sections were deparaffinized in xylene and rehydrated followed by antigen retrieval in 10 mM sodium citrate and a blocking step with 10% normal donkey serum/5% BSA/PBS. Chicken anti-GFP (Abcam), rabbit anti-*Salmonella* O4 antigen (Abcam), rat anti-LAMP1 (Developmental Studies Hybridoma Bank), rabbit anti-cleaved caspase-3 (Cell Signaling), rabbit anti-cleaved caspase-8 (Cell Signaling), rat anti-PMN (Ly6-6B2, SeroTec) and mouse anti-E-cadherin (BD Transduction Laboratories) antibodies as well as the indicated fluorophore-conjugated secondary antibodies (Jackson ImmunoResearch) were used. Fluorescein-conjugated (Vector) or AF647-conjugated (Invitrogen) Wheat Germ Agglutinin (WGA) was used to detect the mucus layer. Slides were subsequently mounted in DAPI mounting medium (Vector) and images were taken using a Zeiss Apo-Tome.2 system microscope connected to a Axiocam 506 digital camera. Images were formatted using the ZEN 2.3 imaging software.

Flow cytometry analysis

For immune cell isolation, the intestine was cut longitudinally and incubated 2x15min in 2mM EDTA/HBSS at 37°C to remove the epithelium. The lamina propria was digested in 30 μ g/ml Liberase/DNAse (Roche) for 45min at 37°C and filtered through a 100 μ m nylon cell strainer to obtain a single cell suspension. The following antibodies from Biolegend were used for the FACS analysis: CD45-BV510 (30-F11), Ly6C-PerCPCy5.5 (HK1.4), Ly6G-PE (1A8), CD11b-APCCy7 (M1/70), MHCII-AF488 (M5/115.14.2). Data were acquired with a BD FACS Canto II and analyzed with FlowJo X.

Transmission electron microscopy

1-day-old MyD88^{+/+} and MyD88^{-/-} mice were infected with wild type *S. Typhimurium* and sacrificed at day 4 p.i.. Tissue samples were prepared for ultrastructural analysis as previously described [88]. After embedding, samples were post-fixed with 1% osmium tetroxide and contrasted with 2% uranyl acetate, both for 2 h. Samples were dehydrated with a graded ethanol series, followed by infiltration with epoxy resin and overnight heat polymerization. Thin, 70 nm sections were prepared using an ultramicrotome Ultracut UCT (Leica Microsystems) and contrasted with 0.2% lead citrate. Sections were analyzed with a JEM-1400 TEM microscope (Jeol) and images were recorded with TemCam-F216 camera using EM MENU software (both Tvips).

Statistical analysis

The One-way ANOVA Kruskal-Wallis test (with Dunn's posttest) and the Mann-Whitney test were employed for statistical analysis of bacterial counts in organ tissue and the comparative transcriptional analysis. Mortality was analyzed by log-rank (Mantel-Cox) test. The GraphPad Prism Software 5.0 was used for statistical evaluation. p values are indicated as follows:

***p<0.001; **p<0.01, and *p<0.05.

Supporting information

S1 Fig. Comparative analysis of the role of SPII-T3SS effector molecules SopA, SopB, SipA and SopE₂ by complementation of *sopABE₂sipA* quadruple mutant *Salmonella*. 1-day-old C57BL/6 mice were orally infected with 100 CFU wild type (WT) pWSK (filled circles), quadruple mutant Δ *sopABE₂sipA* pWSK (open circles), Δ *sopABE₂sipA* *psopA* (inverted open triangles), Δ *sopABE₂sipA* *psopB* (open triangles), Δ *sopABE₂sipA* *psipA* (open squares), or Δ *sopABE₂sipA* *psopE₂* (open diamonds) *S. Typhimurium*. Viable counts in (A) isolated gentamicin-treated enterocytes at 4 days post infection (p.i.). (B) Quantitative RT-PCR for *Cxcl2* and (C) *Cxcl5* mRNA in total RNA prepared from enterocytes isolated at 4 days p.i.. Values were normalized to uninfected age-matched control animals (crosses). Viable counts in (D) total MLN homogenate, (E) total liver tissue homogenate and (F) total spleen tissue homogenate at 4 days post infection (p.i.). Individual values and the mean from at least two independent experiments are shown (n = 5–8 animals per group). (G) Immunostaining for *Salmonella* (red) in small intestinal tissue sections at 4 days p.i. with 100 CFU WT pWSK, Δ *sopABE₂sipA* pWSK, Δ *sopABE₂sipA* *psopA*, Δ *sopABE₂sipA* *psopB*, Δ *sopABE₂sipA* *psipA*, or Δ *sopABE₂sipA* *psopE₂* *S. Typhimurium*. Counterstaining with E-cadherin (green), WGA (white) and DAPI (blue). Bar, 5 μ m. (H) A confluent monolayer of polarized murine intestinal epithelial m-IC_{cl2} cells were infected at a multiplicity of infection (MOI) of 1:10 with WT pWSK, SPII mutant Δ *invC*, Δ *sopABE₂sipA* pWSK, Δ *sopABE₂sipA* *psopA*, Δ *sopABE₂sipA* *psopB*, Δ *sopABE₂sipA* *psipA*, or Δ *sopABE₂sipA* *psopE₂* *S. Typhimurium* for 1 h at 37°C. Cells were subsequently treated with 100 μ g/mL gentamicin for 1 h at 37°C, washed three times, and lysed in 0.1% Triton X-100. The number of viable bacteria in cell lysates and inoculi was determined by serial dilution and plating. The number of intracellular, gentamicin-protected bacteria relative to the inoculum is shown (%). Results represent the mean \pm SD. (TIF)

S2 Fig. Comparative analysis of the role of SPII-T3SS effector molecules SopE₂ and SopE by complementation of *sopABE₂sipA* quadruple mutant *Salmonella*. 1-day-old C57BL/6 mice were orally infected with 100 CFU WT pWSK (filled circles), Δ *sopABE₂sipA* pWSK (open circles), Δ *sopABE₂sipA* *psopE₂* (open diamonds), or Δ *sopABE₂sipA* *psopE* (half-filled diamonds) *S. Typhimurium*. Viable counts in (A) isolated gentamicin-treated enterocytes at 4 days p.i.. (B) Quantitative RT-PCR for *Cxcl2* and (C) *Cxcl5* mRNA in total RNA prepared from enterocytes isolated at 4 days p.i.. Values were normalized to uninfected age-matched control animals (crosses). Viable counts in (D) total MLN homogenate, (E) total liver tissue homogenate, and (F) total spleen tissue homogenate at 4 days p.i.. Individual values and the mean from at least two independent experiments are shown (n = 5–8 animals per group). (G) Immunostaining for *Salmonella* (red) in small intestinal tissue sections at 4 days p.i. with 100 CFU WT pWSK or Δ *sopABE₂sipA* *psopE* *S. Typhimurium*. Counterstaining with E-cadherin (green), WGA (white) and DAPI (blue). Bar, 5 μ m. (H) Gentamicin protection assay (as described under (H)) was performed with WT pWSK, Δ *sopABE₂sipA* pWSK, Δ *sopABE₂sipA* *psopE₂*, or Δ *sopABE₂sipA* *psopE*. The number of intracellular, gentamicin-protected bacteria relative to the inoculum is shown (%). Results represent the mean \pm SD. (TIF)

S3 Fig. Comparative analysis of the role of SPII-T3SS effector molecules SopA, SopB, SipA, or SopE₂ using triple mutants. (A–C) 1-day-old C57BL/6 mice were orally infected with 100 CFU WT (filled circles), *sopABE₂sipA* quadruple mutant (open circles), *sopBE₂sipA* (inverted open triangles), *sopAE₂sipA* (open triangles), *sopABE₂* (open squares), or *sopABsipA* mutant (open diamonds) *S. Typhimurium*. Viable counts in (A) MLN and (B) total spleen

tissue homogenate at 4 days post infection (p.i.). (C) Quantitative RT-PCR for *Cxcl5* mRNA in total RNA prepared from enterocytes isolated at 4 days p.i.. Values were normalized to uninfected age-matched control animals (crosses). Individual values and the mean from at least two independent experiments are shown (n = 5–8 animals per group). (D) Gentamicin protection assay (as described in S1H Fig) was performed using WTpWSK, $\Delta invC$, $\Delta sopABE_2sipA$, $\Delta sopBE_2sipA$, $\Delta sopAE_2sipA$, $\Delta sopABE_2$, or $\Delta sopABsipA$ *S. Typhimurium*. The number of intracellular, gentamicin-protected bacteria relative to the inoculum is shown (%). Results represent the mean \pm SD.

(TIF)

S4 Fig. The influence of MyD88-dependent innate immune signaling on intraepithelial microcolony formation. (A and B) 1-day-old MyD88^{+/+} and MyD88^{-/-} mice were left untreated or orally infected with 100 CFU wild type *S. Typhimurium*. Relative expression of (A) *Cxcl2* and (B) *Cxcl5* mRNA in total RNA prepared from enterocytes isolated from non-infected and infected MyD88^{+/+} mice as well as non-infected and infected MyD88^{-/-} mice at 4 days p.i. were measured by quantitative RT-PCR. Relative expression from at least two independent experiments are shown (n = 2–6 animals per group). The data for MyD88^{+/+} animals infected with *S. Typhimurium* WT are identical to Fig 1C and S3C Fig. (C) Survival following *S. Typhimurium* infection. 1-day-old MyD88^{+/+} (n = 12; solid line) and MyD88^{-/-} (n = 12; broken line) mice were orally infected with 100 CFU WT *S. Typhimurium* (broken line). Animals that had to be euthanized due to a rise in the clinical score were included in the analysis (see material and methods).

(TIF)

S5 Fig. The role of SipA and SopE₂ for systemic spread and innate immune stimulation. (A–C) 1-day-old C57BL/6 mice were orally infected with 100 CFU WT (filled circles) or $\Delta sopE_2sipA$ *S. Typhimurium* (filled triangles). Viable counts in (A) MLN and (B) total spleen tissue homogenate at 4 days p.i.. (C) Quantitative RT-PCR for *Cxcl5* mRNA in total RNA prepared from enterocytes isolated at 4 days p.i.. Values were normalized to uninfected age-matched control animals (crosses). Individual values and the mean from at least two independent experiments are shown (n = 3–5 animals per group). (D–F) 1-day-old C57BL/6 mice were orally infected with 100 CFU WT (filled circles) $\Delta sipA$ (open squares), $\Delta sipA$ complemented with *psipA* (filled squares), $\Delta sopE_2$ (open diamonds), or $\Delta sopE_2$ complemented with *psopE_2* (filled diamonds) *S. Typhimurium*. Viable counts in (D) MLN and (E) total spleen tissue homogenate at 4 days p.i.. (F) Quantitative RT-PCR for *Cxcl5* mRNA in total RNA prepared from enterocytes isolated at 4 days p.i.. Values were normalized to uninfected age-matched control animals (crosses). Individual values and the mean from at least two independent experiments are shown (n = 3–7 animals per group). The data for uninfected control animals and *Salmonella* WT infected mice are identical to S3A–S3C Fig.

(TIF)

S6 Fig. The role of SopB/SopE₂ and SopA/SopE₂ for systemic spread and innate immune stimulation. (A–C) 1-day-old C57BL/6 mice were orally infected with 100 CFU WT (filled circles), $\Delta sopBE_2$ (inverted open triangles), or $\Delta sopAE_2$ (open triangles) *S. Typhimurium*. Viable counts in (A) MLN and (B) total spleen tissue homogenate at 4 days p.i.. (C) Quantitative RT-PCR for *Cxcl5* mRNA in total RNA prepared from enterocytes isolated at 4 days p.i.. Values were normalized to uninfected age-matched control animals (crosses). Individual values and the mean from at least two independent experiments are shown (n = 3–8 animals per group). The data for uninfected control animals and *Salmonella* WT infected mice are identical to S3A–S3C Fig.

(TIF)

S7 Fig. The role of SopB for systemic spread and innate immune stimulation. (A and B) 1-day-old C57BL/6 mice were orally infected with 100 CFU wild type (WT) (filled circles), Δ sopB (filled triangles), or Δ sopB psopB (open triangles) *S. Typhimurium*. Viable counts in (A) total spleen tissue homogenate at 2 days post infection (p.i.). (B) Quantitative RT-PCR for *Cxcl5* mRNA in total RNA prepared from enterocytes isolated at 2 days p.i.. Values were normalized to uninfected age-matched control animals (crosses). Individual values and the mean from at least two independent experiments are shown (n = 3–5 animals per group). (C) Immunostaining for cleaved caspase 3 (cl. caspase 3, upper panel, red) and cleaved caspase 8 (cl. caspase 8, lower panel, red) in small intestinal tissue sections from healthy age-matched control animals (non-infected) or at 3 days p.i. with WT, Δ sopB and Δ sopB psopB *S. Typhimurium*. Counterstaining with E-cadherin (green), and DAPI (blue). Bar, 50 μ m. (TIF)

S8 Fig. SipA exerts a proinflammatory, disease-promoting influence. (A) Postnatal body weight gain of healthy and infected animals. 1-day-old C57BL/6 mice were left untreated (solid line) or orally infected with 100 CFU WT (broken line) or Δ sopABE₂ *S. Typhimurium* (dotted line). (B) Survival following *S. Typhimurium* infection. 1-day-old C57BL/6 mice were orally infected with 100 CFU WT (solid line), Δ sopABE₂ (broken line), or sipA^{K635A E637W} Δ sopABE₂ *S. Typhimurium* (broken line). Animals that had to be euthanized due to a rise in the clinical score were included in the analysis (see [material and methods](#)). (C) Total length (in cm) of the small intestine at 4 days p.i. and of uninfected age-matched control animals. 1-day-old C57BL/6 mice were infected with 100 CFU WT, Δ sopBE₂sipA (inverted open triangles), Δ sopAE₂sipA (open triangles) Δ sopABE₂ (open squares) and or Δ sopABsipA (open diamonds) *S. Typhimurium*. Individual values and the mean from at least two independent experiments are shown (n = 3–5 animals per group). (D) Mucosal barrier integrity tested by serum quantification 4 hours after oral administration of FITC labeled-4kDa dextran. 1-day-old C57BL/6 mice were infected with WT (filled circles), Δ sopABsipA (open diamonds), or Δ sopAE₂sipA (open triangles) *S. Typhimurium*. FITC labeled-4 kDa dextran was quantified in serum at day 4 p.i.. (E and F) Flow cytometric analysis of lamina propria immune cells. 1-day-old mice were orally infected with 100 CFU WT, Δ sopAE₂sipA, Δ sopABsipA, or Δ sopABE₂ *S. Typhimurium* and total SI leukocytes were analyzed by flow cytometry at day 4 p.i.. (E) Monocytes (Ly6C^{hi}Ly6G⁻CD11b⁺MHCII^{lo/-}CD45⁺DAPI⁻) and (F) neutrophils (Ly6G⁺Ly6C^{int}CD11b⁺MHCII^{lo/-}CD45⁺DAPI⁻) are depicted as % of CD45⁺ cells. The results represent the mean values from at least two independent experiments (n = 4–6 per group). (G and H) Quantitative analysis (G) and immunostaining (H) of PMN infiltrating the small intestinal tissue. PMN from 10–20 image fields obtained from neonates infected with wild type (WT), Δ sipA, Δ sipA psipA, Δ sipA psipA^{D434A} *S. Typhimurium* (n = 3–9) and uninfected age-matched control animals (n = 5) were analyzed at day 4 p.i.. Values and mean are shown. Bar, 25 μ m. (I) Viable counts in isolated gentamicin-treated enterocytes at 2 days p.i. of 1-day-old mice with 100 CFU WT (filled circle), Δ sopABE₂ (open squares), or sipA^{K635A E637W} Δ sopABE₂ *S. Typhimurium* (filled squares). Values and mean from at least two independent experiments are shown (n = 4–6 animals per group). (TIF)

S9 Fig. The role of SipA for intraepithelial microcolony formation. (A–C) 1-day-old C57BL/6 mice were orally infected with 100 CFU WT (filled circles), Δ sipA (open diamonds), Δ sipA complemented with psipA^{K635A E637W} (half-filled diamonds), Δ sipA complemented with psipA^{D434A} (filled squares), or Δ sipA complemented with psipA^{D434A K635A E637W} (filled triangles) *S. Typhimurium*. Viable counts in (A) MLN and (B) total spleen tissue homogenate at 4 days p.i.. (C) Quantitative RT-PCR for *Cxcl5* mRNA in total RNA prepared from enterocytes isolated at 4 days p.i.. Values were normalized to uninfected age-matched control animals

(crosses). Individual values and the mean from at least two independent experiments are shown ($n = 4-7$ animals per group). The data for uninfected control animals and *Salmonella* WT infected mice are identical to [S3A–S3C Fig. \(D\)](#) Survival following *S. Typhimurium* infection. 1-day-old C57BL/6 mice were orally infected with 100 CFU WT (solid line), $\Delta sipA$ (broken line), or $\Delta sipA$ complemented with $sipA^{K635A E637W}$ (broken line) *S. Typhimurium*. Animals that had to be euthanized due to a rise in the clinical score were included in the analysis (see [Material and Methods](#)).

(TIF)

S1 Table. *Salmonella enterica* serovar Typhimurium strains and plasmids used in this study. Strain name, designation, genotype description and reference are listed for all strains and plasmids used in the study.

(DOCX)

S2 Table. Oligonucleotides used in this study. Oligonucleotide name and sequence are listed for all oligonucleotides used in the study.

(DOC)

S3 Table. Phenotype of *Salmonella* mutants. Summary of the results obtained in this study using all bacterial mutants indicating the genotype, the time point of the analysis and the phenotype, namely enterocyte invasion, LAMP1 recruitment to the *Salmonella* microcolony, SPI2 T3SS reporter activation, transcriptional stimulation of the intestinal epithelium, intraepithelial proliferation and spread to spleen and liver tissue.

(DOC)

Acknowledgments

We gratefully acknowledge the technical support from Dominique Gütle, Thorben Albers, Regina Holland and Josephine Weber-Heynemann. We thank the Electron Microscopy Laboratory at the Department of Biosciences, University of Oslo.

Author Contributions

Conceptualization: Kaiyi Zhang, Ambre Riba, Monika Nietschke, Natalia Torow, Urska Repnik, Marcus Fulde, Aline Dupont, Michael Hensel, Mathias Hornef.

Data curation: Kaiyi Zhang, Ambre Riba, Monika Nietschke, Natalia Torow, Urska Repnik, Andreas Pütz.

Formal analysis: Kaiyi Zhang.

Funding acquisition: Marcus Fulde, Michael Hensel, Mathias Hornef.

Investigation: Kaiyi Zhang, Ambre Riba, Monika Nietschke, Natalia Torow, Urska Repnik, Andreas Pütz.

Methodology: Kaiyi Zhang, Natalia Torow, Urska Repnik, Mathias Hornef.

Project administration: Mathias Hornef.

Resources: Michael Hensel, Mathias Hornef.

Supervision: Mathias Hornef.

Validation: Kaiyi Zhang, Natalia Torow, Urska Repnik, Michael Hensel, Mathias Hornef.

Visualization: Kaiyi Zhang, Ambre Riba, Natalia Torow, Urska Repnik.

Writing – original draft: Kaiyi Zhang, Mathias Hornef.

Writing – review & editing: Kaiyi Zhang, Aline Dupont, Michael Hensel.

References

1. Coburn B, Grassl GA, Finlay BB. Salmonella, the host and disease: a brief review. *Immunol Cell Biol*. 2007; 85(2):112–8. <https://doi.org/10.1038/sj.icb.7100007> PMID: 17146467.
2. Majowicz SE, Musto J, Scallan E, Angulo FJ, Kirk M, O'Brien SJ, et al. The global burden of nontyphoidal Salmonella gastroenteritis. *Clinical infectious diseases: an official publication of the Infectious Diseases Society of America*. 2010; 50(6):882–9. <https://doi.org/10.1086/650733> PMID: 20158401.
3. Milledge J, Calis JC, Graham SM, Phiri A, Wilson LK, Soko D, et al. Aetiology of neonatal sepsis in Blantyre, Malawi: 1996–2001. *Annals of tropical paediatrics*. 2005; 25(2):101–10. <https://doi.org/10.1179/146532805X45692> PMID: 15949198.
4. Feasey NA, Dougan G, Kingsley RA, Heyderman RS, Gordon MA. Invasive non-typhoidal salmonella disease: an emerging and neglected tropical disease in Africa. *Lancet*. 2012; 379(9835):2489–99. [https://doi.org/10.1016/S0140-6736\(11\)61752-2](https://doi.org/10.1016/S0140-6736(11)61752-2) PMID: 22587967; PubMed Central PMCID: PMC3402672.
5. LaRock DL, Chaudhary A, Miller SI. Salmonellae interactions with host processes. *Nature reviews Microbiology*. 2015; 13(4):191–205. <https://doi.org/10.1038/nrmicro3420> PMID: 25749450.
6. Que F, Wu S, Huang R. Salmonella pathogenicity island 1(SPI-1) at work. *Current microbiology*. 2013; 66(6):582–7. <https://doi.org/10.1007/s00284-013-0307-8> PMID: 23370732.
7. Laughlin RC, Knodler LA, Barhoumi R, Payne HR, Wu J, Gomez G, et al. Spatial segregation of virulence gene expression during acute enteric infection with *Salmonella enterica* serovar Typhimurium. *mBio*. 2014; 5(1):e00946–13. <https://doi.org/10.1128/mBio.00946-13> PMID: 24496791; PubMed Central PMCID: PMC3950517.
8. Agbor TA, McCormick BA. Salmonella effectors: important players modulating host cell function during infection. *Cellular microbiology*. 2011; 13(12):1858–69. <https://doi.org/10.1111/j.1462-5822.2011.01701.x> PMID: 21902796; PubMed Central PMCID: PMC3381885.
9. Zhou D, Mooseker MS, Galan JE. Role of the *S. typhimurium* actin-binding protein SipA in bacterial internalization. *Science*. 1999; 283(5410):2092–5. PMID: 10092234.
10. Zhou D, Mooseker MS, Galan JE. An invasion-associated Salmonella protein modulates the actin-bundling activity of plastin. *Proceedings of the National Academy of Sciences of the United States of America*. 1999; 96(18):10176–81. PMID: 10468582; PubMed Central PMCID: PMC17862.
11. Lilic M, Galkin VE, Orlova A, VanLoock MS, Egelman EH, Stebbins CE. Salmonella SipA polymerizes actin by stapling filaments with nonglobular protein arms. *Science*. 2003; 301(5641):1918–21. <https://doi.org/10.1126/science.1088433> PMID: 14512630.
12. Lee CA, Silva M, Siber AM, Kelly AJ, Galyov E, McCormick BA. A secreted Salmonella protein induces a proinflammatory response in epithelial cells, which promotes neutrophil migration. *Proceedings of the National Academy of Sciences of the United States of America*. 2000; 97(22):12283–8. <https://doi.org/10.1073/pnas.97.22.12283> PMID: 11050248; PubMed Central PMCID: PMC17333.
13. Wood MW, Jones MA, Watson PR, Siber AM, McCormick BA, Hedges S, et al. The secreted effector protein of *Salmonella dublin*, SopA, is translocated into eukaryotic cells and influences the induction of enteritis. *Cellular microbiology*. 2000; 2(4):293–303. PMID: 11207586.
14. Layton AN, Brown PJ, Galyov EE. The Salmonella translocated effector SopA is targeted to the mitochondria of infected cells. *Journal of bacteriology*. 2005; 187(10):3565–71. <https://doi.org/10.1128/JB.187.10.3565-3571.2005> PMID: 15866946; PubMed Central PMCID: PMC1112013.
15. Zhang Y, Higashide WM, McCormick BA, Chen J, Zhou D. The inflammation-associated Salmonella SopA is a HECT-like E3 ubiquitin ligase. *Molecular microbiology*. 2006; 62(3):786–93. <https://doi.org/10.1111/j.1365-2958.2006.05407.x> PMID: 17076670.
16. Galyov EE, Wood MW, Rosqvist R, Mullan PB, Watson PR, Hedges S, et al. A secreted effector protein of *Salmonella dublin* is translocated into eukaryotic cells and mediates inflammation and fluid secretion in infected ileal mucosa. *Molecular microbiology*. 1997; 25(5):903–12. PMID: 9364916.
17. Norris FA, Wilson MP, Wallis TS, Galyov EE, Majerus PW. SopB, a protein required for virulence of *Salmonella dublin*, is an inositol phosphate phosphatase. *Proceedings of the National Academy of Sciences of the United States of America*. 1998; 95(24):14057–9. PMID: 9826652; PubMed Central PMCID: PMC3424325.

18. Terebiznik MR, Vieira OV, Marcus SL, Slade A, Yip CM, Trimble WS, et al. Elimination of host cell PtdIns(4,5)P(2) by bacterial SigD promotes membrane fission during invasion by Salmonella. *Nat Cell Biol.* 2002; 4(10):766–73. <https://doi.org/10.1038/ncb854> PMID: 12360287.
19. Zhou D, Chen LM, Hernandez L, Shears SB, Galan JE. A Salmonella inositol polyphosphatase acts in conjunction with other bacterial effectors to promote host cell actin cytoskeleton rearrangements and bacterial internalization. *Molecular microbiology.* 2001; 39(2):248–59. PMID: 11136447.
20. Steele-Mortimer O, Knodler LA, Marcus SL, Scheid MP, Goh B, Pfeifer CG, et al. Activation of Akt/protein kinase B in epithelial cells by the Salmonella typhimurium effector sigD. *The Journal of biological chemistry.* 2000; 275(48):37718–24. <https://doi.org/10.1074/jbc.M008187200> PMID: 10978351.
21. Knodler LA, Finlay BB, Steele-Mortimer O. The Salmonella effector protein SopB protects epithelial cells from apoptosis by sustained activation of Akt. *The Journal of biological chemistry.* 2005; 280(10):9058–64. <https://doi.org/10.1074/jbc.M412588200> PMID: 15642738.
22. Wood MW, Rosqvist R, Mullan PB, Edwards MH, Galyov EE. SopE, a secreted protein of Salmonella dublin, is translocated into the target eukaryotic cell via a sip-dependent mechanism and promotes bacterial entry. *Molecular microbiology.* 1996; 22(2):327–38. PMID: 8930917.
23. Hardt WD, Chen LM, Schuebel KE, Bustelo XR, Galan JE. S. typhimurium encodes an activator of Rho GTPases that induces membrane ruffling and nuclear responses in host cells. *Cell.* 1998; 93(5):815–26. PMID: 9630225.
24. Stender S, Friebel A, Linder S, Rohde M, Mirol S, Hardt WD. Identification of SopE2 from Salmonella typhimurium, a conserved guanine nucleotide exchange factor for Cdc42 of the host cell. *Molecular microbiology.* 2000; 36(6):1206–21. PMID: 10931274.
25. Takeuchi A. Electron microscope studies of experimental Salmonella infection. I. Penetration into the intestinal epithelium by Salmonella typhimurium. *The American journal of pathology.* 1967; 50(1):109–36. PMID: 5334433; PubMed Central PMCID: PMC1965174.
26. Giannella RA, Formal SB, Dammin GJ, Collins H. Pathogenesis of salmonellosis. Studies of fluid secretion, mucosal invasion, and morphologic reaction in the rabbit ileum. *The Journal of clinical investigation.* 1973; 52(2):441–53. <https://doi.org/10.1172/JCI107201> PMID: 4630603; PubMed Central PMCID: PMC302274.
27. Nietfeld JC, Tyler DE, Harrison LR, Cole JR, Latimer KS, Crowell WA. Invasion of enterocytes in cultured porcine small intestinal mucosal explants by Salmonella choleraesuis. *American journal of veterinary research.* 1992; 53(9):1493–9. PMID: 1416346.
28. Muller AJ, Kaiser P, Dittmar KE, Weber TC, Haueter S, Endt K, et al. Salmonella gut invasion involves TTSS-2-dependent epithelial traversal, basolateral exit, and uptake by epithelium-sampling lamina propria phagocytes. *Cell host & microbe.* 2012; 11(1):19–32. <https://doi.org/10.1016/j.chom.2011.11.013> PMID: 22264510.
29. Sellin ME, Muller AA, Felmy B, Dolowschiak T, Diard M, Tardivel A, et al. Epithelium-intrinsic NAIP/NLRC4 inflammasome drives infected enterocyte expulsion to restrict Salmonella replication in the intestinal mucosa. *Cell host & microbe.* 2014; 16(2):237–48. <https://doi.org/10.1016/j.chom.2014.07.001> PMID: 25121751.
30. Tsois RM, Adams LG, Ficht TA, Baumler AJ. Contribution of Salmonella typhimurium virulence factors to diarrheal disease in calves. *Infection and immunity.* 1999; 67(9):4879–85. PMID: 10456944; PubMed Central PMCID: PMC96822.
31. Tsois RM, Adams LG, Hantman MJ, Scherer CA, Kimbrough T, Kingsley RA, et al. SspA is required for lethal Salmonella enterica serovar Typhimurium infections in calves but is not essential for diarrhea. *Infection and immunity.* 2000; 68(6):3158–63. PMID: 10816458; PubMed Central PMCID: PMC97552.
32. Zhang S, Santos RL, Tsois RM, Stender S, Hardt WD, Baumler AJ, et al. The Salmonella enterica serotype typhimurium effector proteins SipA, SopA, SopB, SopD, and SopE2 act in concert to induce diarrhea in calves. *Infection and immunity.* 2002; 70(7):3843–55. <https://doi.org/10.1128/IAI.70.7.3843-3855.2002> PMID: 12065528; PubMed Central PMCID: PMC96822.
33. Zhang S, Adams LG, Nunes J, Khare S, Tsois RM, Baumler AJ. Secreted effector proteins of Salmonella enterica serotype typhimurium elicit host-specific chemokine profiles in animal models of typhoid fever and enterocolitis. *Infection and immunity.* 2003; 71(8):4795–803. <https://doi.org/10.1128/IAI.71.8.4795-4803.2003> PMID: 12874363; PubMed Central PMCID: PMC96822.
34. Zhang S, Kingsley RA, Santos RL, Andrews-Polymenis H, Raffatellu M, Figueiredo J, et al. Molecular pathogenesis of Salmonella enterica serotype typhimurium-induced diarrhea. *Infection and immunity.* 2003; 71(1):1–12. <https://doi.org/10.1128/IAI.71.1.1-12.2003> PMID: 12496143; PubMed Central PMCID: PMC96822.
35. Barthel M, Hapfelmeier S, Quintanilla-Martinez L, Kremer M, Rohde M, Hogardt M, et al. Pretreatment of mice with streptomycin provides a Salmonella enterica serovar Typhimurium colitis model that allows

- analysis of both pathogen and host. *Infection and immunity*. 2003; 71(5):2839–58. <https://doi.org/10.1128/IAI.71.5.2839-2858.2003> PMID: 12704158; PubMed Central PMCID: PMC153285.
36. Lawhon SD, Khare S, Rossetti CA, Everts RE, Galindo CL, Luciano SA, et al. Role of SPI-1 secreted effectors in acute bovine response to *Salmonella enterica* Serovar Typhimurium: a systems biology analysis approach. *PloS one*. 2011; 6(11):e26869. <https://doi.org/10.1371/journal.pone.0026869> PMID: 22096503; PubMed Central PMCID: PMC3214023.
 37. Anjum MF, Marooney C, Fookes M, Baker S, Dougan G, Ivens A, et al. Identification of core and variable components of the *Salmonella enterica* subspecies I genome by microarray. *Infection and immunity*. 2005; 73(12):7894–905. <https://doi.org/10.1128/IAI.73.12.7894-7905.2005> PMID: 16299280; PubMed Central PMCID: PMC1307019.
 38. Ochman H, Groisman EA. Distribution of pathogenicity islands in *Salmonella* spp. *Infection and immunity*. 1996; 64(12):5410–2. PMID: 8945597; PubMed Central PMCID: PMC174539.
 39. Hartmann H, Meyer H, Koch H, Steinbach G, Gunther H. [Salmonellosis in the calf. 1. development of an infection model and experiments on pathogenesis]. *Arch Exp Veterinarmed*. 1973; 27(2):289–300. PMID: 4725027.
 40. Jones MA, Wood MW, Mullan PB, Watson PR, Wallis TS, Galyov EE. Secreted effector proteins of *Salmonella dublin* act in concert to induce enteritis. *Infection and immunity*. 1998; 66(12):5799–804. PMID: 9826357; PubMed Central PMCID: PMC108733.
 41. Zhang S, Santos RL, Tsois RM, Mirold S, Hardt WD, Adams LG, et al. Phage mediated horizontal transfer of the *sopE1* gene increases enteropathogenicity of *Salmonella enterica* serotype Typhimurium for calves. *FEMS Microbiol Lett*. 2002; 217(2):243–7. PMID: 12480111.
 42. Raffatellu M, Wilson RP, Chessa D, Andrews-Polymeris H, Tran QT, Lawhon S, et al. SipA, SopA, SopB, SopD, and SopE2 contribute to *Salmonella enterica* serotype typhimurium invasion of epithelial cells. *Infection and immunity*. 2005; 73(1):146–54. <https://doi.org/10.1128/IAI.73.1.146-154.2005> PMID: 15618149; PubMed Central PMCID: PMC538951.
 43. Smith BP, Habasha F, Reina-Guerra M, Hardy AJ. Bovine salmonellosis: experimental production and characterization of the disease in calves, using oral challenge with *Salmonella typhimurium*. *American journal of veterinary research*. 1979; 40(11):1510–3. PMID: 393144.
 44. Frost AJ, Bland AP, Wallis TS. The early dynamic response of the calf ileal epithelium to *Salmonella typhimurium*. *Veterinary pathology*. 1997; 34(5):369–86. <https://doi.org/10.1177/030098589703400501> PMID: 9381648.
 45. Santos RL, Zhang S, Tsois RM, Baumler AJ, Adams LG. Morphologic and molecular characterization of *Salmonella typhimurium* infection in neonatal calves. *Veterinary pathology*. 2002; 39(2):200–15. <https://doi.org/10.1354/vp.39-2-200> PMID: 12009058.
 46. Bolton AJ, Martin GD, Osborne MP, Wallis TS, Stephen J. Invasiveness of *Salmonella* serotypes Typhimurium, Choleraesuis and Dublin for rabbit terminal ileum *in vitro*. *Journal of medical microbiology*. 1999; 48(9):801–10. <https://doi.org/10.1099/00222615-48-9-801> PMID: 10482290.
 47. Bolton AJ, Osborne MP, Wallis TS, Stephen J. Interaction of *Salmonella choleraesuis*, *Salmonella dublin* and *Salmonella typhimurium* with porcine and bovine terminal ileum *in vivo*. *Microbiology*. 1999; 145(Pt 9):2431–41. <https://doi.org/10.1099/00221287-145-9-2431> PMID: 10517596.
 48. Jones BD, Ghori N, Falkow S. *Salmonella typhimurium* initiates murine infection by penetrating and destroying the specialized epithelial M cells of the Peyer's patches. *The Journal of experimental medicine*. 1994; 180(1):15–23. PMID: 8006579; PubMed Central PMCID: PMC2191576.
 49. Martinez-Argudo I, Jepson MA. *Salmonella* translocates across an *in vitro* M cell model independently of SPI-1 and SPI-2. *Microbiology*. 2008; 154(Pt 12):3887–94. <https://doi.org/10.1099/mic.0.2008/021162-0> PMID: 19047755.
 50. Zhang K, Dupont A, Torow N, Gohde F, Leschner S, Lienenklaus S, et al. Age-dependent enterocyte invasion and microcolony formation by *Salmonella*. *PLoS pathogens*. 2014; 10(9):e1004385. <https://doi.org/10.1371/journal.ppat.1004385> PMID: 25210785; PubMed Central PMCID: PMC4161480.
 51. Hapfelmeier S, Ehrbar K, Stecher B, Barthel M, Kremer M, Hardt WD. Role of the *Salmonella* pathogenicity island 1 effector proteins SipA, SopB, SopE, and SopE2 in *Salmonella enterica* subspecies 1 serovar Typhimurium colitis in streptomycin-pretreated mice. *Infection and immunity*. 2004; 72(2):795–809. <https://doi.org/10.1128/IAI.72.2.795-809.2004> PMID: 14742523; PubMed Central PMCID: PMC321604.
 52. Hapfelmeier S, Stecher B, Barthel M, Kremer M, Muller AJ, Heikenwalder M, et al. The *Salmonella* pathogenicity island (SPI)-2 and SPI-1 type III secretion systems allow *Salmonella* serovar typhimurium to trigger colitis via MyD88-dependent and MyD88-independent mechanisms. *Journal of immunology*. 2005; 174(3):1675–85. PMID: 15661931.
 53. Knodler LA, Crowley SM, Sham HP, Yang H, Wrande M, Ma C, et al. Noncanonical inflammasome activation of caspase-4/caspase-11 mediates epithelial defenses against enteric bacterial pathogens. *Cell*

- host & microbe. 2014; 16(2):249–56. <https://doi.org/10.1016/j.chom.2014.07.002> PMID: 25121752; PubMed Central PMCID: PMC4157630.
54. Mirol S, Rabsch W, Rohde M, Stender S, Tschape H, Russmann H, et al. Isolation of a temperate bacteriophage encoding the type III effector protein SopE from an epidemic *Salmonella typhimurium* strain. Proceedings of the National Academy of Sciences of the United States of America. 1999; 96(17):9845–50. PMID: 10449782; PubMed Central PMCID: PMC22298.
 55. Bakshi CS, Singh VP, Wood MW, Jones PW, Wallis TS, Galyov EE. Identification of SopE2, a *Salmonella* secreted protein which is highly homologous to SopE and involved in bacterial invasion of epithelial cells. Journal of bacteriology. 2000; 182(8):2341–4. PMID: 10735884; PubMed Central PMCID: PMC111290.
 56. Patel JC, Galan JE. Differential activation and function of Rho GTPases during *Salmonella*-host cell interactions. The Journal of cell biology. 2006; 175(3):453–63. <https://doi.org/10.1083/jcb.200605144> PMID: 17074883; PubMed Central PMCID: PMC2064522.
 57. Friebel A, Ilchmann H, Aepfelbacher M, Ehrbar K, Machleidt W, Hardt WD. SopE and SopE2 from *Salmonella typhimurium* activate different sets of RhoGTPases of the host cell. The Journal of biological chemistry. 2001; 276(36):34035–40. <https://doi.org/10.1074/jbc.M100609200> PMID: 11440999.
 58. Madan R, Rastogi R, Parashuraman S, Mukhopadhyay A. *Salmonella* acquires lysosome-associated membrane protein 1 (LAMP1) on phagosomes from Golgi via SipC protein-mediated recruitment of host Syntaxin6. The Journal of biological chemistry. 2012; 287(8):5574–87. <https://doi.org/10.1074/jbc.M111.286120> PMID: 22190682; PubMed Central PMCID: PMC3285332.
 59. Deiwick J, Nikolaus T, Erdogan S, Hensel M. Environmental regulation of *Salmonella* pathogenicity island 2 gene expression. Molecular microbiology. 1999; 31(6):1759–73. PMID: 10209748.
 60. Arpaia N, Godec J, Lau L, Sivick KE, McLaughlin LM, Jones MB, et al. TLR signaling is required for *Salmonella typhimurium* virulence. Cell. 2011; 144(5):675–88. <https://doi.org/10.1016/j.cell.2011.01.031> PMID: 21376231; PubMed Central PMCID: PMC3063366.
 61. Bens M, Bogdanova A, Cluzeaud F, Miquero L, Kerneis S, Kraehenbuhl JP, et al. Transimmortalized mouse intestinal cells (m-ICc12) that maintain a crypt phenotype. The American journal of physiology. 1996; 270(6 Pt 1):C1666–74. <https://doi.org/10.1152/ajpcell.1996.270.6.C1666> PMID: 8764149.
 62. Chuang TH, Hahn KM, Lee JD, Danley DE, Bokoch GM. The small GTPase Cdc42 initiates an apoptotic signaling pathway in Jurkat T lymphocytes. Mol Biol Cell. 1997; 8(9):1687–98. PMID: 9307966; PubMed Central PMCID: PMC305729.
 63. Hoffmann C, Galle M, Dilling S, Kappeli R, Muller AJ, Songhet P, et al. In macrophages, caspase-1 activation by SopE and the type III secretion system-1 of *S. typhimurium* can proceed in the absence of flagellin. PloS one. 2010; 5(8):e12477. <https://doi.org/10.1371/journal.pone.0012477> PMID: 20814576; PubMed Central PMCID: PMC2930008.
 64. Agbor TA, Demma Z, Mrsny RJ, Castillo A, Boll EJ, McCormick BA. The oxido-reductase enzyme glutathione peroxidase 4 (GPX4) governs *Salmonella Typhimurium*-induced neutrophil transepithelial migration. Cellular microbiology. 2014; 16(9):1339–53. <https://doi.org/10.1111/cmi.12290> PMID: 24617613; PubMed Central PMCID: PMC4146641.
 65. Wall DM, Nadeau WJ, Pazos MA, Shi HN, Galyov EE, McCormick BA. Identification of the *Salmonella enterica* serotype typhimurium SipA domain responsible for inducing neutrophil recruitment across the intestinal epithelium. Cellular microbiology. 2007; 9(9):2299–313. <https://doi.org/10.1111/j.1462-5822.2007.00960.x> PMID: 17697195.
 66. Srikanth CV, Wall DM, Maldonado-Contreras A, Shi H, Zhou D, Demma Z, et al. *Salmonella* pathogenesis and processing of secreted effectors by caspase-3. Science. 2010; 330(6002):390–3. <https://doi.org/10.1126/science.1194598> PMID: 20947770; PubMed Central PMCID: PMC4085780.
 67. Li D, Wang X, Wang L, Zhou D. The actin-polymerizing activity of SipA is not essential for *Salmonella enterica* serovar Typhimurium-induced mucosal inflammation. Infection and immunity. 2013; 81(5):1541–9. <https://doi.org/10.1128/IAI.00337-12> PMID: 23439302; PubMed Central PMCID: PMC3648018.
 68. Hallstrom KN, Srikanth CV, Agbor TA, Dumont CM, Peters KN, Paraoan L, et al. PERP, a host tetra-spanning membrane protein, is required for *Salmonella*-induced inflammation. Cellular microbiology. 2015; 17(6):843–59. <https://doi.org/10.1111/cmi.12406> PMID: 25486861; PubMed Central PMCID: PMC4915744.
 69. Andritschke D, Dilling S, Emmenlauer M, Welz T, Schmich F, Misselwitz B, et al. A Genome-Wide siRNA Screen Implicates Spire 1/2 in SipA-Driven *Salmonella Typhimurium* Host Cell Invasion. PloS one. 2016; 11(9):e0161965. <https://doi.org/10.1371/journal.pone.0161965> PMID: 27627128; PubMed Central PMCID: PMC45023170.

70. Piscatelli HL, Li M, Zhou D. Dual 4- and 5-phosphatase activities regulate SopB-dependent phosphoinositide dynamics to promote bacterial entry. *Cellular microbiology*. 2016; 18(5):705–19. <https://doi.org/10.1111/cmi.12542> PMID: 26537021.
71. Hanisch J, Kolm R, Wozniczka M, Bumann D, Rottner K, Stradal TE. Activation of a RhoA/myosin II-dependent but Arp2/3 complex-independent pathway facilitates *Salmonella* invasion. *Cell host & microbe*. 2011; 9(4):273–85. <https://doi.org/10.1016/j.chom.2011.03.009> PMID: 21501827.
72. Humphreys D, Davidson A, Hume PJ, Koronakis V. *Salmonella* virulence effector SopE and Host GEF ARNO cooperate to recruit and activate WAVE to trigger bacterial invasion. *Cell host & microbe*. 2012; 11(2):129–39. <https://doi.org/10.1016/j.chom.2012.01.006> PMID: 22341462; PubMed Central PMCID: PMC3314957.
73. Steele-Mortimer O, Brummell JH, Knodler LA, Meresse S, Lopez A, Finlay BB. The invasion-associated type III secretion system of *Salmonella enterica* serovar Typhimurium is necessary for intracellular proliferation and vacuole biogenesis in epithelial cells. *Cellular microbiology*. 2002; 4(1):43–54. PMID: 11856172.
74. Brawn LC, Hayward RD, Koronakis V. *Salmonella* SPI1 effector SipA persists after entry and cooperates with a SPI2 effector to regulate phagosome maturation and intracellular replication. *Cell host & microbe*. 2007; 1(1):63–75. <https://doi.org/10.1016/j.chom.2007.02.001> PMID: 18005682; PubMed Central PMCID: PMC331885946.
75. Mallo GV, Espina M, Smith AC, Terebiznik MR, Aleman A, Finlay BB, et al. SopB promotes phosphatidylinositol 3-phosphate formation on *Salmonella* vacuoles by recruiting Rab5 and Vps34. *The Journal of cell biology*. 2008; 182(4):741–52. <https://doi.org/10.1083/jcb.200804131> PMID: 18725540; PubMed Central PMCID: PMC332518712.
76. Bakowski MA, Braun V, Lam GY, Yeung T, Heo WD, Meyer T, et al. The phosphoinositide phosphatase SopB manipulates membrane surface charge and trafficking of the *Salmonella*-containing vacuole. *Cell host & microbe*. 2010; 7(6):453–62. <https://doi.org/10.1016/j.chom.2010.05.011> PMID: 20542249.
77. Vonaesch P, Sellin ME, Cardini S, Singh V, Barthel M, Hardt WD. The *Salmonella* Typhimurium effector protein SopE transiently localizes to the early SCV and contributes to intracellular replication. *Cellular microbiology*. 2014; 16(12):1723–35. <https://doi.org/10.1111/cmi.12333> PMID: 25052734.
78. Kamanova J, Sun H, Lara-Tejero M, Galan JE. The *Salmonella* Effector Protein SopA Modulates Innate Immune Responses by Targeting TRIM E3 Ligase Family Members. *PLoS pathogens*. 2016; 12(4): e1005552. <https://doi.org/10.1371/journal.ppat.1005552> PMID: 27058235; PubMed Central PMCID: PMC4825927.
79. Keestra AM, Winter MG, Klein-Douwel D, Xavier MN, Winter SE, Kim A, et al. A *Salmonella* virulence factor activates the NOD1/NOD2 signaling pathway. *mBio*. 2011; 2(6). <https://doi.org/10.1128/mBio.00266-11> PMID: 22186610; PubMed Central PMCID: PMC33238304.
80. Chen LM, Bagrodia S, Cerione RA, Galan JE. Requirement of p21-activated kinase (PAK) for *Salmonella* typhimurium-induced nuclear responses. *The Journal of experimental medicine*. 1999; 189(9):1479–88. PMID: 10224288; PubMed Central PMCID: PMC332193063.
81. Bruno VM, Hannemann S, Lara-Tejero M, Flavell RA, Kleinstein SH, Galan JE. *Salmonella* Typhimurium type III secretion effectors stimulate innate immune responses in cultured epithelial cells. *PLoS pathogens*. 2009; 5(8):e1000538. <https://doi.org/10.1371/journal.ppat.1000538> PMID: 19662166; PubMed Central PMCID: PMC332714975.
82. Silva M, Song C, Nadeau WJ, Matthews JB, McCormick BA. *Salmonella* typhimurium SipA-induced neutrophil transepithelial migration: involvement of a PKC- α -dependent signal transduction pathway. *American journal of physiology Gastrointestinal and liver physiology*. 2004; 286(6):G1024–31. <https://doi.org/10.1152/ajpgi.00299.2003> PMID: 14739142.
83. Hu GQ, Song PX, Chen W, Qi S, Yu SX, Du CT, et al. Critical role for *Salmonella* effector SopB in regulating inflammasome activation. *Mol Immunol*. 2017; 90:280–6. <https://doi.org/10.1016/j.molimm.2017.07.011> PMID: 28846926.
84. Ruan H, Zhang Z, Tian L, Wang S, Hu S, Qiao JJ. The *Salmonella* effector SopB prevents ROS-induced apoptosis of epithelial cells by retarding TRAF6 recruitment to mitochondria. *Biochem Biophys Res Commun*. 2016; 478(2):618–23. <https://doi.org/10.1016/j.bbrc.2016.07.116> PMID: 27473656.
85. Verheij M, Bose R, Lin XH, Yao B, Jarvis WD, Grant S, et al. Requirement for ceramide-initiated SAPK/JNK signalling in stress-induced apoptosis. *Nature*. 1996; 380(6569):75–9. <https://doi.org/10.1038/380075a0> PMID: 8598911.
86. Hoffmann S, Schmidt C, Walter S, Bender JK, Gerlach RG. Scarless deletion of up to seven methyl-accepting chemotaxis genes with an optimized method highlights key function of CheM in *Salmonella* Typhimurium. *PloS one*. 2017; 12(2):e0172630. <https://doi.org/10.1371/journal.pone.0172630> PMID: 28212413; PubMed Central PMCID: PMC5315404.

87. Lotz M, Gutle D, Walther S, Menard S, Bogdan C, Hornef MW. Postnatal acquisition of endotoxin tolerance in intestinal epithelial cells. *The Journal of experimental medicine*. 2006; 203(4):973–84. <https://doi.org/10.1084/jem.20050625> PMID: 16606665; PubMed Central PMCID: PMC2118301.
88. Dupont A, Sommer F, Zhang K, Repnik U, Basic M, Bleich A, et al. Age-Dependent Susceptibility to Enteropathogenic *Escherichia coli* (EPEC) Infection in Mice. *PLoS pathogens*. 2016; 12(5):e1005616. <https://doi.org/10.1371/journal.ppat.1005616> PMID: 27159323; PubMed Central PMCID: PMC4861285.
89. Hurley BP, Sin A, McCormick BA. Adhesion molecules involved in heparin A3-mediated neutrophil transepithelial migration. *Clin Exp Immunol*. 2008; 151(2):297–305. <https://doi.org/10.1111/j.1365-2249.2007.03551.x> PMID: 18005361; PubMed Central PMCID: PMC2276941.